



TALLINNA TEHNIKAÜLIKOOL
TALLINN UNIVERSITY OF TECHNOLOGY

DEPARTMENT OF MATERIALS AND
ENVIRONMENTAL TECHNOLOGY

TiO₂ THIN FILMS BY ULTRASONIC SPRAY PYROLYSIS
TiO₂ ÕHUKESED KILED ULTRAHELI PIHUSTUSPÜROLÜÜSI MEETODIL
MASTER THESIS

Student: Zengjun Chen
/name/

Student code:165555KAYM.....

Supervisor: ...Ilona Oja Acik, Senior Researcher;
Ibrahim DüNDAR, Early Stage Researcher
/name, position/

Tallinn, 2018

AUTHOR'S DECLARATION

Hereby I declare, that I have written this thesis independently.

No academic degree has been applied for based on this material. All works, major viewpoints and data of the other authors used in this thesis have been referenced.

“.....” 201.....

Author:

/signature /

Thesis is in accordance with terms and requirements

“.....” 201....

Supervisor:

/signature/

Accepted for defence

“.....”201....

Chairman of theses defence commission:

/name and signature/

THESIS TASK

Student:Zengjun Chen, 165555KAYM.....(name, student code)

Study programme, ...KAYM09/09 Materials and Processes for Sustainable Energetics.... (code and title)

main speciality: Materials for sustainable energetics

Supervisor(s): Senior research scientist, Ilona Oja Acik, +372 620 3369; Early stage researcher, Ibrahim Dündar, +372 54628958... (position, name, phone)

Consultants:(name, position)

..... (company, phone, e-mail)

Thesis topic:

(in English) *..TiO₂ thin films by ultrasonic spray pyrolysis..*

(in Estonian) ...TiO₂ õhukesed kiled ultraheli pihustuspirolüüsi meetodil.....

Thesis main objectives:

1. To deposited TiO₂ thin films by ultrasonic spray pyrolysis on glass, Si, ITO coated glass substrates at different deposition temperature.
2. To analyse the structural, optical and electrical properties of TiO₂ thin films.
3. To measure the performance of the TiO₂ solar cells.

Thesis tasks and time schedule:

No	Task description	Deadline
1.	To deposited TiO ₂ thin films on glass and Si substrates at different deposition temperature and anneal at different temperature.	19.10.2017
2.	To analyse the structural, optical and electrical properties of TiO ₂ thin films and to measure the performance of the TiO ₂ solar cells	12.02.2018
3.	To write the master thesis	25.05.2018

Language: ...English... **Deadline for submission of thesis:** “.....”201.... a

Student: ...Zengjun Chen.. “.....”201....a

/signature/

Supervisor: ...Ilona Oja Acik. “.....”201....a

/signature/

Consultant: “.....”201....a

/signature/

Terms of thesis closed defence and/or restricted access conditions to be formulated on the reverse side

CONTENTS

1. INTRODUCTION.....	9
2. BACKGROUND AND LITERATURE REVIEW.....	11
2.1. Titanium dioxide.....	11
2.2. TiO ₂ thin films by chemical deposition methods.....	12
2.2.1. Properties of TiO ₂ thin films by chemical deposition method.....	13
2.2.2. Influence of annealing process for TiO ₂ thin films.....	15
2.3. Chemical Spray pyrolysis method.....	15
2.3.1. Pneumatic spray pyrolysis method.....	16
2.3.2. Advantages and disadvantages of pneumatic spray pyrolysis method.....	17
2.3.3. Ultrasonic spray pyrolysis method.....	17
2.3.4. Advantages and disadvantages of ultrasonic spray pyrolysis method.....	18
2.4. Applications of TiO ₂ thin films.....	19
2.4.1. TiO ₂ thin films in solar cells.....	20
2.5. Summary of literature review.....	23
2.6. Aim of the thesis.....	23
3. METHODOLOGY.....	25
3.1. Chemicals.....	25
3.2. The preparation of spray solution.....	25
3.3. Substrates.....	27
3.4. USP apparatus and parameters.....	27
3.5. Deposition of TiO ₂ thin films.....	28

3.6. Annealing of TiO ₂ thin films.....	29
3.7. Testing of TiO ₂ thin films in hybrid solar cell structure.....	30
3.8. Characterization methods.....	30
3.8.1. X-ray Diffraction.....	30
3.8.2. Raman Spectroscopy.....	31
3.8.3. UV-visible spectroscopy.....	31
3.8.4. Current-voltage measurements.....	31
4. RESULTS AND DISCUSSIONS.....	33
4.1. Optical properties of TiO ₂ thin films.....	33
4.1.1. Total Transmittance of TiO ₂ thin films deposited onto glass substrates.....	33
4.1.2. Thicknesses of the TiO ₂ thin films on glass and Si substrates.....	35
4.1.3. The band gap of TiO ₂ thin films deposited onto glass substrates.....	38
4.2. Structural properties of TiO ₂ thin films.....	40
4.2.1. XRD results of TiO ₂ thin films deposited on glass substrates.....	40
4.2.2. XRD results of TiO ₂ thin films deposited on Si substrates.....	41
4.2.3. Raman results of TiO ₂ thin films deposited on glass substrates.....	45
4.2.4. Raman results of TiO ₂ thin films deposited on Si substrates.....	46
4.3. Electrical properties of TiO ₂ thin films.....	48
4.3.1. The electrical resistivity of TiO ₂ thin films deposited on glass substrates.....	48
4.3.2. Electrical resistivity of TiO ₂ thin films deposited on Si substrates.....	49
4.4. Solar cell properties.....	51
5. SUMMARY.....	55

5. ACKNOWLEDGEMENTS..... 57

6. LIST OF REFERENCES..... 58

7. APPENDICES..... 66

PREFACE

Firstly, I would like to thank my supervisor Ilona Oja Acik, senior research scientist of the Laboratory of Thin Films Chemical Technologies, Department of Material Science who gave me this topic and guided me through all the experiments and writing of my thesis. Whenever I had question, she was very patient to solve it. It's a great pleasure to work in the Laboratory of Thin Films Chemical Technologies with all stuffs. Secondly, my special thanks to my co-supervisor, Ibrahim Dündar, PhD student in Laboratory of Thin Films Chemical Technologies, who was very patient to explain all my questions and taught me to operate all the experiments and results analysis. Also, I am very thankful to Mr. Arvo Mere who helped me the electrical measurements and Dr. Atanas Katerski who helped me make the solar cells and measure the performances.

In present work, we have studied the structural, optical and electrical properties of TiO₂ thin films deposited by ultrasonic spray pyrolysis at different substrates temperature for solar cell applications. The films were sprayed from solution containing titanium(IV) isopropoxide, acetylacetone in molar ratio of 1:4 in ethanol and deposited onto substrate of microscopy glass, n-type Si (100) wafer at temperatures of 200 to 500 °C and indium tin oxide coated glass substrates at 300 °C and 400 °C for solar cell. The resulting films were annealed at 500 °C and 700 °C for 1 hour in air. The films were characterized by UV-vis spectroscopy, XRD, Raman, and I-V measurements. Results showed that the total transmittance of TiO₂ thin films decreased after annealing. The annealed film thickness increased from 80 to 510 nm with increasing deposition temperature from 200 to 500 °C. Band gap for TiO₂ thin films decreased from 3.5 to 3.2 eV as the deposition temperature increased from 200 to 500 °C. As deposited films prepared below 500 °C were amorphous, whereas crystalline anatase films were obtained at 500 °C. Further annealing at 700 °C in air led to anatase crystalline formation when films were deposited below 500 °C whereas the films deposited at 500 °C consist of anatase and rutile phases. The results of the fabricated solar cells with a structure of ITO/TiO₂/P3HT/Au show better performance of TiO₂ solar cell which was deposited at 400 °C rather than 300 °C due to the increased V_{oc} was from 390 mV to 460 mV.

Keywords: TiO₂, ultrasonic spray pyrolysis, thin films, structural properties.

List of abbreviations and symbols

A- absorbance

AcacH- acetylacetone

ACA- anthracene-9-carboxylic acid

CSP- chemical spray pyrolysis

Cu- copper

CVD- chemical vapor deposition

d- thickness

E_g - band gap energy

EtoH- ethanol

GW- gigawatts

ITO-indium doped tin oxide

PV- photovoltaics

Si-silicon

T -transmission

TiO₂- titanium oxide

TTIP- titanium isopropoxide

USP- ultrasonic spray pyrolysis

UV- ultraviolet

XRD-x-ray diffraction

α - absorption coefficient

1. INTRODUCTION

The increase in world population and energy consumption has caused an increase in CO₂ emissions and the rapid depletion of fossil fuels. The environmental problems have become a major issue. It is reported that oil resources will decline significantly in the next 40 years[1]. Considering the rate of current energy consumption, it is expected that oil reserves will last for 42 years, natural gas reserves will be 60 years, and coal reserves will be 130 years which are very scarce in the future [2].

Therefore, in order to ensure a sustainable supply of world energy demand, the need for renewable and environmentally friendly alternative energy sources is necessary.

There are many sources of energy that are renewable and considered to be environmentally friendly. For instance, tidal, solar, wind, hydro, geothermal, biomass, nuclear. Among all the alternative energy, solar energy has received great attention due to its applicability, potential and free use of sunlight. Solar cells showed high potential in the world cumulative installation. The growth of solar PV capacity is the fastest, increasing from 2004 (3.7 GW) to 2014 (177 GW), an increase of 48 times [3]. In 2016, PV capacity increased by at least 75 GW, and new installed capacity increased by 50% year-on-year. By the end of this year, cumulative installed capacity reached at least 302 GW, enough to provide 1.8% of the world's total electricity consumption. At the same time, solar cells become more efficient, portable and more flexible, making installation simple.

Of all semiconducting metal oxides used in solar PV, TiO₂ nanomaterials seem to be a significant candidate because its chemical and optical stability, non-toxic, low cost, and corrosion resistance.

TiO₂ is a typical wide band gap semiconductor, indicating its suitability for use in electronic and photonic materials such as transparent conductor and transistor applications. Recently, photocatalytic properties have been extensively studied for applications involving water purification and self-cleaning, particularly photovoltaic applications. It has been used for dye-sensitized [4], organic [5], and perovskite [6] solar cells, which play an important role in solar energy production.

In this thesis, TiO₂ thin films were deposited on the microscopy glass, Si and ITO substrates by using ultrasonic spray pyrolysis method. The aim of this work is to deposit TiO₂ thin films at different substrate temperature and to investigate its structural, optical and electrical properties for solar cell

applications. The films were characterized by UV-vis spectroscopy, XRD, Raman, and I-V measurements.

2. BACKGROUND AND LITERATURE REVIEW

2.1. Titanium dioxide

Titanium dioxide, also known as titanium oxide (IV) or titanium dioxide, is a naturally occurring titanium oxide with the chemical formula TiO_2 . Due to its chemical stability, non-toxicity, photoelectric properties, low cost and high photocatalytic performance, TiO_2 has become an increasingly important material in the last decades. Titanium dioxide (TiO_2) has three crystalline polymorphs: rutile (tetragonal), brookite (orthorhombic), and anatase (tetragonal) [7], all three crystal structures consisting of distorted TiO_6 octahedra are shown in Fig. 2.1. In general, rutile is thermodynamically stable at high temperatures. The anatase phase is metastable and irreversibly converted to rutile at elevated temperatures [8]. The brookite phase is the rarest of the natural TiO_2 polymorphs and is the most difficult phase to prepare in the laboratory. The band gap is reported at 3.0 eV for rutile and 3.2 eV for anatase [9].

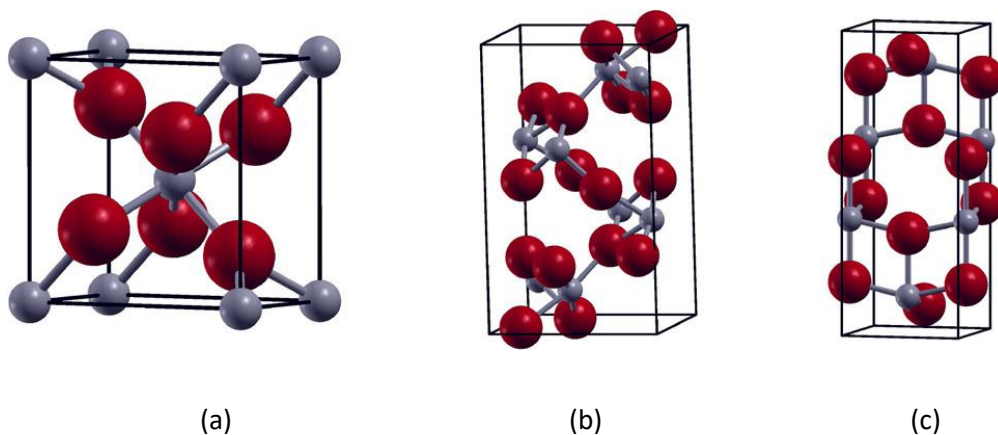


Figure 2.1 Crystal structures of TiO_2 : (a) rutile, (b) brookite, (c) anatase [10]

Since TiO_2 thin film with anatase phase has a wide band gap (3.2 eV), only UV radiation range can be used in photocatalytic process, but its high transparency is suitable for coating on glass [11] and small grain size provides high surface area for photocatalysis [12]. However, rutile phase has lower band gaps (3.0 eV), which is possible to utilize both UV and visible light in photocatalytic processes,

but rutile phase is grown in higher temperature which leads to the disadvantages of larger grain size, lower surface area and lower transparency [13].

In generally, the anatase structure is more preferred than other polymorphs used in solar cells because anatase phase has a larger band gap, potentially higher conduction band edge energy and lower electron-hole pair recombination rate [14].

2.2. TiO₂ thin films by chemical deposition methods

The chemical deposition methods are summarized in Fig. 2.2. In general, the chemical method can be divided as gas phase deposition methods and methods with solution precursors.

The gas phase methods contain chemical vapour deposition (CVD) and atomic layer epitaxy (ALE). While sol-gel, dip coating, spin coating and spray pyrolysis are solution-based methods.

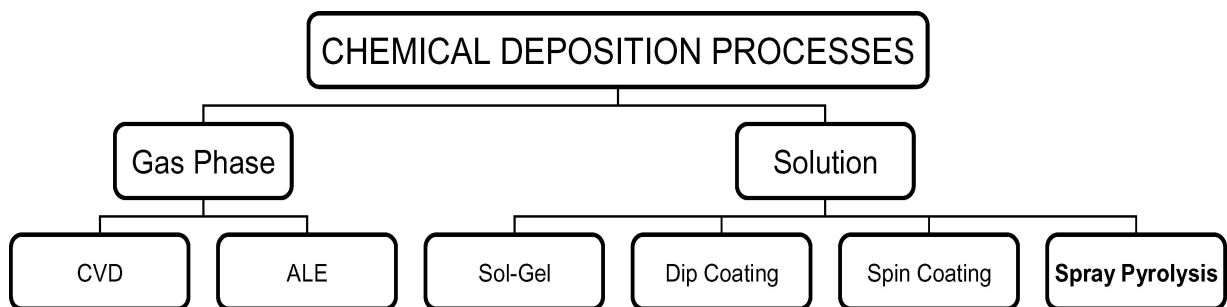


Figure 2.2 Chemical deposition method of thin films [15]

TiO₂ films have been deposited by many chemical methods, including sol-gel spin coating [16,20], spray pyrolysis [21], chemical vapour deposition [22]. In recent years, spray pyrolysis method is considered to be one of the most promising methods for preparing TiO₂ thin films. Spray pyrolysis methods are pneumatic spray pyrolysis [26] and ultrasonic spray pyrolysis [25,27].

2.2.1. Properties of TiO₂ thin films by chemical deposition method

Various methods have been used for the deposition of TiO₂ thin films. The most used methods are sol-gel spin coating and chemical spray pyrolysis. TiO₂ thin films were mostly sprayed on glass, Si, quarts and ITO substrates.

It is reported that TiO₂ thin films deposited by sol-gel spin coating method showed amorphous structure when deposition temperature is below 300 °C, whereas anatase crystal structure is observed at deposition temperature above 300 °C. Annealing process at higher temperatures will change the structure of film from amorphous to anatase phase. Further annealing at above 700 °C can transform anatase phase to rutile phase [16]-[21].

It is also reported that TiO₂ thin films deposited by spray pyrolysis method mostly showed anatase phase at deposition temperature above 400 °C. The results of annealing process at different temperature showed pure anatase phase, mixture phase of anatase and rutile phases and pure rutile phase respectively. Band gap also varies with deposition and annealing temperature [23]-[27].

The summary of the properties of TiO₂ thin film by different methods are listed in Table 2.1.

Table 2.1 Summary of TiO₂ films deposited by chemical methods

Deposition method	Precursor	Solvent	Substrate	Ts (°C)	Tan (°C)	Results of TiO ₂ properties			Ref
						Crystal structure	Band gap (eV)	Resistivity (Ω·cm)	
Spin coating	TiCl ₃	NH ₄ OH	glass	25	300	Ts: amorphous		-	[16]
Sol-gel spin coating	titanium (IV) butoxide	ethanol	glass	25	500	Ts: amorphous Tan: anatase		Ts: 2.34E+04 Tan: 3.20E+03	[17]
Sol-gel spin coating	titanium (IV) butoxide	ethanol.	glass	60	700	Tan: anatase + rutile	Tan: 3.24 -	Ts: 2.34E+04 Tan: 3.20E+03	[18]

Sol-gel spin coating	titanium (IV) butoxide	ethanol	glass	25	500	Ts: amorphous, Tan: anatase	Tan: 3.78	4.5E+09	[19]
Sol-gel spin coating	titanium (IV) butoxide	ethanol	Si	25	300, 500, 700, 900	Ts: amorphous, 300<Tan<700: anatase, Tan=900: anatase +rutile	-	Tan=900: 7.19*10 ²	[20]
Spray pyrolysis	titanium (IV) isopropoxide	ethanol	ITO	150-350	350-500	Ts: amorphous, Tan: anatase	-	-	[21]
Chemical vapour deposition	titanium (IV) isopropoxide	ethanol	quartz	250-500	750	anatase	2.99-3.32		[22]
Ultrasonic spray pyrolysis	titanium (IV) isopropoxide	Acetylacetone	Si	420-540	-	anatase	3.28-3.38	-	[23]
Chemical spray pyrolysis	titanium (IV) isopropoxide	glacial acetic acid	Si	400-500	750	Ts: anatase, Tan: rutile	Ts: 3.43 Tan: 3.33		[24]
Ultrasonic spray pyrolysis	titanium (IV) isopropoxide	ethanol	glass	460	-	anatase	3.41		[25]
Pneumatic spray pyrolysis	titanium isopropoxide	ethanol	Si	435	700, 800	Ts: amorphous, Tan=700: anatase, Tan=800: rutile			[26]
Ultrasonic spray pyrolysis	titanium butoxide	methanol	quartz	400	600, 800, 1000	Ts: anatase Tan=600: anatase; Tan=800: anatase + rutile; Tan=1000: rutile	Tan=600: 3.54 Tan=1000: :3.26		[27]

2.2.2. Influence of annealing process for TiO₂ thin films

Annealing process plays an important role for the crystalline structure, optical properties and electrical properties of TiO₂ thin films.

It is reported that annealing process will influence the crystalline structure and increase the crystallite size of TiO₂ thin films. Senain *et al* [17] has reported the crystalline structure of TiO₂ thin film changed from amorphous to anatase phase after annealing at 500 °C by using sol-gel dip coating method. Bakri *et al* has studied TiO₂ thin films by sol-gel dip coating and the crystallite size of TiO₂ films vary from 21 to 26 nm with different annealing temperature from 300 to 900 °C [20].

Annealing process can also remove the organic residuals in TiO₂ thin film and reduce the thickness of film. It is also reported that annealing of TiO₂ thin film can increase surface area, make the film more porous and decreases the transmittance of the film [28]-[30].

2.3. Chemical Spray pyrolysis method

Chemical spray pyrolysis is a process in which a thin film is deposited by spraying a solution onto a heated substrate where the components react to form a chemical compound. Except the desired compound unnecessary solvent will be volatile at deposition temperature. This process is especially useful for the deposition of oxides [31].

This method has been used to deposit powders, dense and porous films, even multilayer films can be easily fabricated using this technology [32]. Spray pyrolysis has been used for decades in the glass industry and solar cell production [33].

The main apparatus of spray pyrolysis equipment are an atomizer, precursor solution, substrate heater, and temperature controller [34].

The following atomizers are usually used in spray pyrolysis technique: air blast (the liquid is exposed to a stream of air), ultrasonic (ultrasonic frequencies produce the short wavelengths necessary for fine atomization) and electrostatic (the liquid is exposed to a high electric field) [35]. Many factors

influence the properties of film, such as: spray rate, substrate temperature, ambient atmosphere, carrier gas, droplet size and also the cooling rate after deposition.

The film thickness depends on the distance between the nozzle and the substrate, the substrate temperature, the concentration of the precursor solution, and the amount of the sprayed precursor solution. The film formation also depends on the process of droplet landing, reaction and solvent evaporation, which are related to droplet size and momentum [36].

Above all these factors, substrate surface temperature is the most important parameter affecting the film roughness, cracking, crystallinity and so on [34].

2.3.1. Pneumatic spray pyrolysis method

Pneumatic spray pyrolysis belongs to chemical spray pyrolysis which uses pneumatic nebulizer to generate small droplets for the deposition of thin films. The major steps for the deposition of thin films by pneumatic spray pyrolysis are summarized below [37]:

- (1) Droplets generated from pneumatic nebulizer.
- (2) Transport of droplets to the heated substrate.
- (3) Surface reaction of droplets and evaporation of solvent.
- (4) Film formation.
- (5) Sintering of the film.

The set-up of pneumatic spray pyrolysis is exhibited in Fig. 2.3.

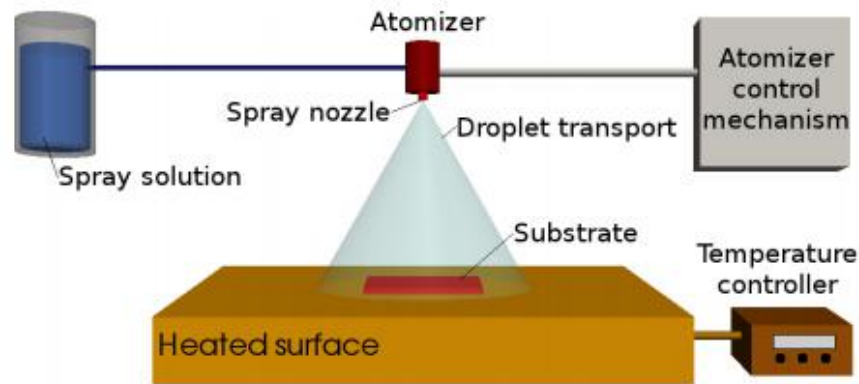


Figure 2.3 Experimental setup of pneumatic spray pyrolysis [37]

2.3.2. Advantages and disadvantages of pneumatic spray pyrolysis method

The advantages of pneumatic spray pyrolysis are listed below [37]-[41] :

- (1) Convenient and simple.
- (2) Inexpensive with cheap equipment and no need for vacuum environment.
- (3) Easy to control the composition and microstructure.
- (4) Can be used for mass production.

However, pneumatic spray pyrolysis has some disadvantages, main ones of can be listed as follows [39]:

- (1) Difficulties with growth temperature determination.
- (2) Hard control of aerosol flow rate.
- (3) Films quality may depend on the droplet size and spray nozzle.

2.3.3. Ultrasonic spray pyrolysis method

Ultrasonic spray pyrolysis is very important method of spray pyrolysis for fabrication on thin films and coatings.

Ultrasonic spray pyrolysis method was used for the deposition of TiO₂ thin film in this study.

In the process of USP, ultrasonic atomizers have been used in order to obtain homogeneously distributed micron sized droplets. Generally, the precursor solution is usually vaporized using an ultrasonic atomizer, the generated fine droplets are transported by the carrier gas to the heated substrate. Director gas is usually needed to adjust the generated aerosol vertically spray on the heated substrate. The solvent will vaporize when the droplets approach the substrate and the reactants will diffuse to the substrate to form thin film [42]. The basic apparatus of ultrasonic spray pyrolysis is shown in Fig. 2.4.

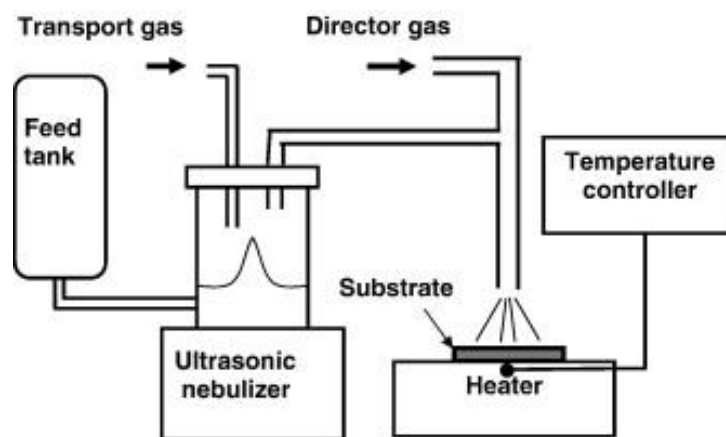


Figure 2.4 typical experimental setup of ultrasonic spray pyrolysis method [43]

2.3.4. Advantages and disadvantages of ultrasonic spray pyrolysis method

USP method is a promising technique, which is considered to be an alternative of chemical vapor deposition.

Besides the advantages mentioned in pneumatic spray pyrolysis, it also has advantages over pneumatic spray pyrolysis which are listed below:

- (1) The gas flow rate of USP is independent of the aerosol flow rate.
- (2) Easier to control the spray flow and deposit thinner and more homogeneous layer.
- (3) The droplet size of the precursor solution is smaller.

(4) The drop size can be decreased by increasing the ultrasonic frequency.

Disadvantages [44]:

(1) low throughput from ultrasonic atomization.

(2) the relationship between the drop size of precursor solution and the particle size of the product is not determined which can influence the size and morphology of the particles produced.

Ultrasonic spray pyrolysis has received considerable attention due to its simplicity, cost-effectiveness, convenience of use, flexibility, absence of vacuum and ease of manufacture.

2.4. Applications of TiO₂ thin films

After the first report by Fujishima and Honda (1972) on the photolysis of water by TiO₂ [45], numerous studies in the properties of nanocrystalline TiO₂ have been generated due to their promising applications in antireflection coatings [46], transparent conductors [47], dielectrics [48], self-cleaning surfaces [49], water purification [50], and in solar cells [4-6].

Due to its chemical stability, low cost, nontoxicity, and high reactivity under UV light irradiation,

TiO₂ has being developed for photocatalytic applications for decades. The main applications are shown in Fig. 2.4.

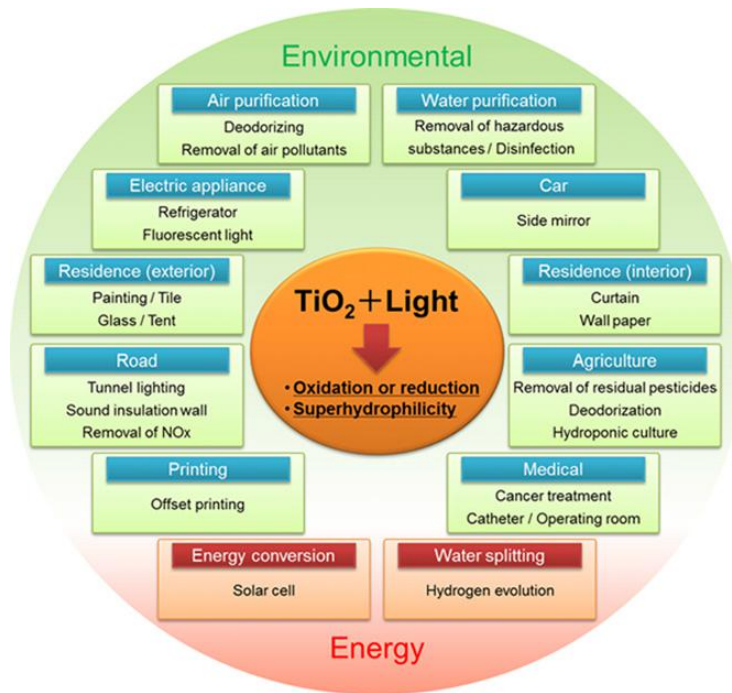


Figure 2.4 Various applications of TiO_2 [51]

2.4.1. TiO_2 thin films in solar cells

Fig. 2.5 shows the structure of dye sensitized solar cell. In dye sensitized solar cell, sensitizer is attached to the surface of the mesoporous TiO_2 film. TiO_2 film is in contact with hole conductor. The working principle of the type of solar cell is:

Photoexcitation of the sensitizer causes electrons to be injected into the conduction band of TiO_2 . TiO_2 can transfer electrons to an electrode. And the electrons finally reach the counter electrode through the circuit. The original state of the sensitizer is restored by the electron supply from the hole conductor.

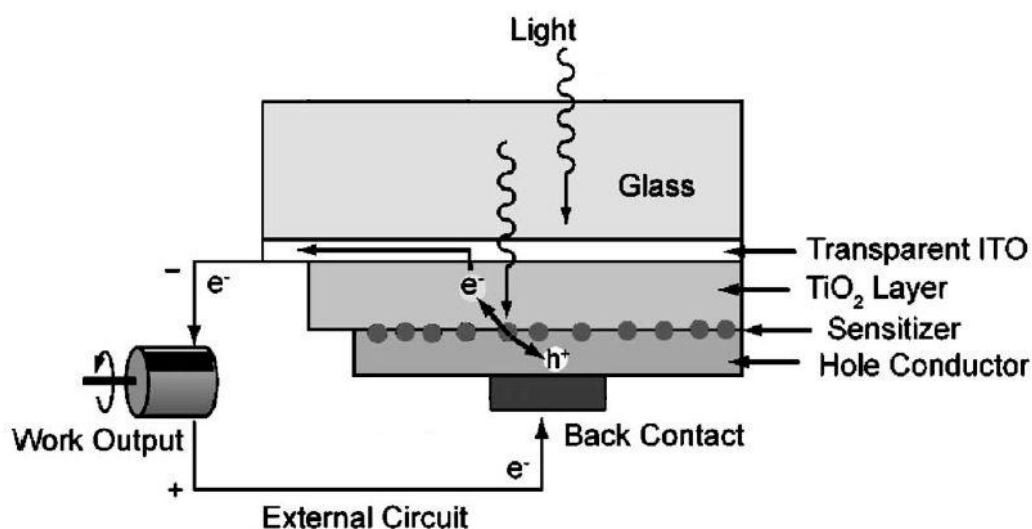


Figure 2.5 the structure of dye sensitized solar cell [50]

TiO₂ has been used in various types of solar cells, including ETA, hybrid, organic, perovskite, dye-sensitized solar cells. The structures and properties of different kinds of solar cells are listed in Table 2.2.

TiO₂ is thermal stable, nontoxic and mesoporous which has high surface area, it has been used as window layer in solar cells.

In a perovskite solar cell with a structure of (Glass/TCO/ETL/Absorber/HTL/Metal), TiO₂ can be used as an electron transporting layer (ETL) due to its high electron mobility. TiO₂ compact layer in perovskite solar cell is used as hole blocking layer (HBL) to avoid the short-circuit problems in the cell by preventing the holes created in the perovskite layer to reach the ITO substrate. Mesoporous TiO₂ is used as a photoanode in dye-sensitized solar cells.

A major challenge of ETA solar cell is low photocurrent conversion efficiency. Porous TiO₂ is used as window layer to increase the absorption of incident light. The improvement of the porosity of TiO₂ is one effective way to increase the photocurrent conversion efficiency of ETA solar cells [52].

Dye-sensitized solar cells have been intensively researched as alternatives to silicon solar cells. TiO₂ is the most common used photoanode materials for dye-sensitized solar cells. Different polymorphs affect the performance of dye-sensitized solar cells. The most common forms of TiO₂ are anatase and

rutile. In general, pure anatase shows higher photovoltaic activity than rutile TiO₂, and the incident photocurrent conversion efficiency mainly depends on the amount of dye loading in anatase TiO₂.

Different types of solar cells have been investigated, the properties of solar cells vary with the structures of the cells. The results are exhibited in Table 2.2, it's found that the value of V_{oc} varies from 0.26 to 1.018 V and efficiency varies from 0.28% to 13.8%.

Table 2.2 Structures and properties of different types of solar cells

Types of solar cells	Structure	Properties				Ref
		J _{sc} (mA/cm ²)	V _{oc} (V)	FF	η (%)	
ETA solar cell	FTO/TiO ₂ /In(OH) ₃ /Pb(OH) _x S _v /Ag	5.75	0.26	0.71	1.06	[52]
Hybrid solar cell	FTO/TiO ₂ /P3HT/ Au	0.41	0.41	0.36	0.06	[53]
Hybrid solar cell	FTO/TiO ₂ /ACA/P3HT/ Au	1.24	0.51	0.43	0.28	[53]
Hybrid solar cell	ITO/TiO ₂ /CuPc/BBOT/Pt	0.17	0.61	0.64	6.51	[54]
Inverted organic solar cell	ITO/TiO ₂ /P3HT:PCBM/MoO ₃ /Ag	8.75	0.52	0.56	2.59	[55]
Perovskite solar cell	FTO/compact-TiO ₂ /mp-TiO ₂ /CH ₃ NH ₃ PbI _{3-x} Cl _x /P3HT/ Au	21.64	0.939	0.62	12.59	[56]
Perovskite solar cell	FTO/compact-TiO ₂ /porous-T iO ₂ /CH ₃ NH ₃ PbI ₃ /NiS-carbon	24.42	0.59	0.36	5.20	[57]
Dye-Sensitized Solar Cell	FTO/TiO ₂ /ruthenium N719 dye/I ⁻ /I ₃ ⁻ /Pt	10.5	570	0.63	4.5	[58]

Dye-Sensitized Solar Cell	FTO/TiO ₂ /silyl-anchor dye/[Co(phen) ₃] ^{3+/2+} / Pt	17.77	1.018	0.765	13.8	[59]
Dye-Sensitized Solar Cell	FTO/TiO ₂ /MAESO (dye)/I ₃ ⁻ /Pt	24.5	0.68	0.55	9.0	[60]

2.5. Summary of literature review

Summaries of literature review are as follow:

- (1) Titanium dioxide (TiO₂) has been shown its attractive chemical, electrical, optical properties as one of the most important semiconductor oxides.
- (2) Various methods have been used for the deposition of TiO₂ thin films. The most used methods are sol-gel spin coating and chemical spray pyrolysis. Besides, annealing process plays an important role for the crystalline structure, optical properties and electrical properties of TiO₂ thin films.
- (3) Ultrasonic Spray Pyrolysis (USP) is one of the important chemical method for fabrication of TiO₂ thin film because of simplicity, cost-effectiveness, convenience of use, flexibility, absence of vacuum and ease of manufacture.
- (4) TiO₂ has been used in various applications related to photocatalysis, including water purification, air purification, self-cleaning glass, medical treatment, water splitting, and solar cells.
- (5) Publications of TiO₂ thin films deposited by ultrasonic spray pyrolysis method are in limited number according to ISI Web of Knowledge database.
- (6) To apply TiO₂ thin films in solar cell device, it is important to understand the properties of the TiO₂ layer.

2.6. Aim of the thesis

The aim of the thesis is to deposit TiO₂ thin films by ultrasonic spray pyrolysis on glass, Si, and indium doped tin oxide (ITO) coated glass substrates at various deposition and annealing temperatures.

To study the structural, optical and electrical properties of TiO₂ thin films deposited by ultrasonic spray pyrolysis.

To study the performance of TiO₂ thin films in the solar cell structure glass /ITO/TiO₂/P3HT.

3. METHODOLOGY

3.1. Chemicals

The chemicals used for the deposition of TiO₂ thin films are listed in Table 3.1.

Table 3.1 Precursors used for the preparation of spray solution for TiO₂ thin films

Deposited materials	Precursor	Formula	Company	Purity
TiO ₂ thin films	Titanium(IV) isopropoxide (TTIP)	C ₁₂ H ₂₈ O ₄ Ti	Merck Schuchardt OHG Germany	≥98%
	Acetylacetone (AcacH)	C ₅ H ₈ O ₂	Merck Schuchardt OHG Germany	≥98%
	Ethanol	C ₂ H ₅ OH	OU Estonian spirit, Estonia	≥96.6%

3.2. The preparation of spray solution

In this work, 0.2 mol/L titanium(IV) isopropoxide solution (50 ml) were used for the deposition of all samples. The chemicals used for preparation of spray solution are titanium(IV) isopropoxide (precursor), acetylacetone (stabilizer) and ethanol (solvent).

The molar ratio of Titanium(IV) isopropoxide (TTIP) and acetylacetone (AcacH) is 1:4. To prepare 50 ml spray solution, 2.96 ml TTIP precursor solution were added in a corked glass bottle firstly, then quickly added AcacH in the bottle and stirred 2 minutes at room temperature. Ethanol as solvent was last added to the bottle and stirred again to make homogeneous solution.

The deposition of TiO₂ thin film was immediately started after the solution was ready. The process of making this solution is schematically showed in Fig. 3.1.

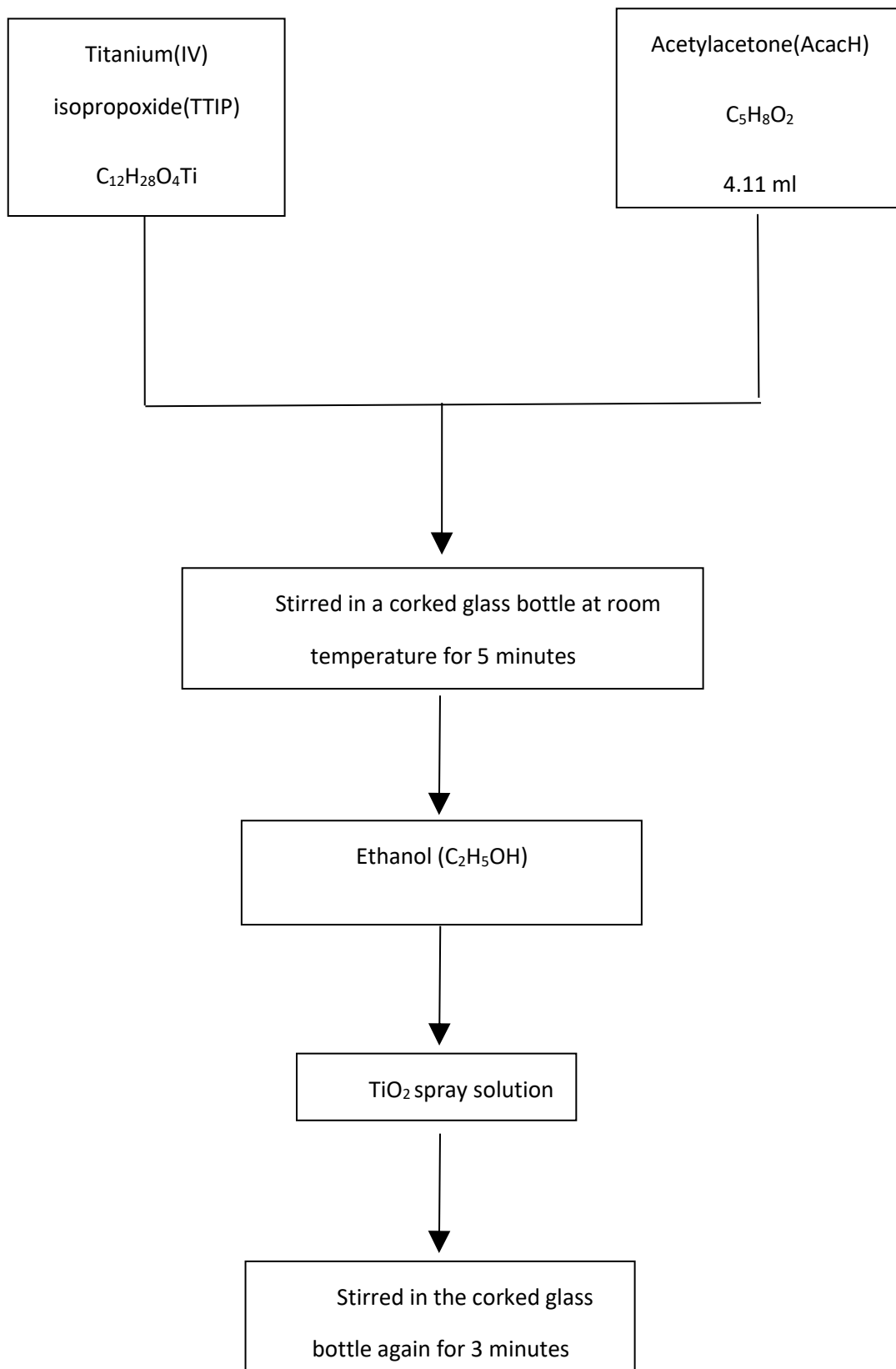


Figure 2.1 The schematic diagram for the preparation of spray solution

3.3. Substrates

Microscopy glass, Si, and Indium doped tin oxide (ITO) coated glass substrates were used for the deposition of TiO₂ thin films.

To remove oil and impurities on the substrates, the substrates were firstly washed with soap solution and rinsed in distilled water for 5 minutes. Then all of the substrates were cleaned in an ultrasonic bath with ethanol for 10 minutes.

Finally, the substrates were dried by compressed air and ready for the spray deposition. The substrates were cut in the dimension of 2.5cm×1.5cm.

3.4. USP apparatus and parameters

The setup of ultrasonic spray pyrolysis is presented in Fig. 3.2. This spray system mainly consists of an ultrasonic generator, air compressor, heater, temperature controller, air flow meter, pipe for transportation of aerosol. The temperature controller can control the temperature of the substrate.

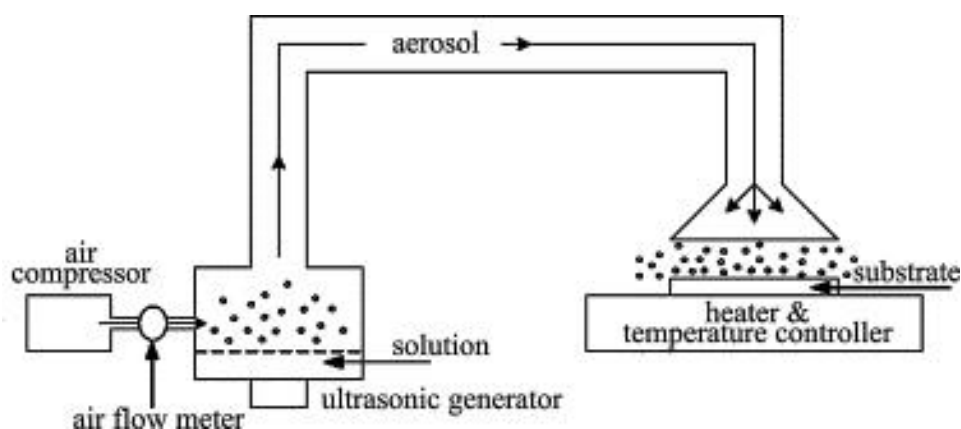


Figure 3.2 Experimental setup for ultrasonic spray pyrolysis [27]

3.5. Deposition of TiO₂ thin films

Before deposition, the substrate was put on the center of the heater; then the deposition temperature was set on a temperature controller which controls the heater. The solution was poured into the ultrasonic generator by a funnel. The spray parameters were set as 2 steps and 6 cycles for deposition of 50 ml solutions.

The carrier gas flow rate and director gas flow rate were set at 5 L/min and 1.2 L/min for the transportation of generated aerosol and the correction of spray direction.

After the heater reached the desired temperature and lasted for 5 minutes for stability, the ultrasonic generator was plugged in to generate aerosol for 2 minutes in order to have enough aerosol for spraying.

Finally, switched on the air controller and started the spray deposition. Deposition parameters of TiO₂ thin films on different substrates are listed in Table 3.2.

Table 3.2 Deposition parameters of the TiO₂ thin film by ultrasonic spray pyrolysis method

Sample name	Substrate	Condition	Substrates temperature (°C)	Carrier gas flow rate (L/min)	Director gas flow rate (L/min)
1.1	glass	0.2 mol/L TTIP solution. 2 steps, 6 cycles	200	5	1.2
1.2	glass		300	5	1.2
1.3	glass		400	5	1.2
1.4	glass		500	5	1.2
2.1	silicon		200	5	1.2
2.2	silicon		300	5	1.2
2.3	silicon		400	5	1.2
2.4	silicon		500	5	1.2
3.1	ITO		300	5	1.2
3.2	ITO		400	5	1.2

3.6. Annealing of TiO₂ thin films

The TiO₂ thin films on glass, Si and ITO substrates deposited at different substrate temperature were annealed at 500 °C in air for 1 hour by using Präzitherm laboratory oven. Firstly, the films were put on the heating plate of the equipment; then the annealing temperature was set up on the temperature controller. After it reached 1 hour of heating at 500 °C, the heater was switched off, and the films were cooled down in room temperature.

Additionally, The TiO₂ thin films on Si substrates deposited at different substrate temperature were also annealed at 700 °C in a Nabertherm L5/11/06D furnace for 1 hour. The films were put in the furnace at first, then the annealing temperature was set as 700 °C and time was set as 1 hour. The heating time up to 700 °C was set as 15 minutes. The films were cooled down in the furnace. The annealing process for different samples is described in Table 3.3.

Table 3.3 Annealing conditions of TiO₂ thin films

Sample name	Substrate	T _s (°C)	T _{an} (°C)	Time (hour)
1.1a	glass	200	500	1
1.2a	glass	300	500	1
1.3a	glass	400	500	1
1.4a	glass	500	500	1
2.1a	Si	200	500	1
2.2a	Si	300	500	1
2.3a	Si	400	500	1
2.4a	Si	500	500	1
2.1b	Si	200	700	1
2.2b	Si	300	700	1
2.3b	Si	400	700	1
2.4b	Si	500	700	1
3.1a	ITO	300	500	1
3.2a	ITO	400	500	1

3.7. Testing of TiO₂ thin films in hybrid solar cell structure

ITO coated glass substrate was used for the deposition of hybrid solar cell. The resistance of the conducting side of the ITO coated glass was measured with a multimeter to be 15–25 Ω on average. The conducting side of the substrate was placed on the front and covered 1/4 of the surface with marble when the substrate was sprayed.

After the deposition and annealing of TiO₂ thin films deposited onto ITO substrates, the next steps were to deposit P3HT as a hole conductor layer and Au as a metal contact. The deposition of P3HT and metal contacts was carried out by Research Scientist, Atanas Katerski in the Laboratory of Thin Film Chemical Technologies.

In order to test different places on the film, several Au contacts (d= 3mm) were deposited on the surface of the TiO₂ thin film.

3.8. Characterization methods

3.8.1. X-ray Diffraction

The structural properties of the samples deposited onto glass and Si substrates was investigated by X-ray diffraction (XRD). A Rigaku Ultima IV diffractometer recorded XRD patterns with Cu K α radiation ($\lambda = 1.5406 \text{ \AA}$, 40 kV at 40 mA).

The measurements were performed in 2 theta configurations with scan range of 20-60°, with a step of 0.02° and a scanning speed of 2°/min. The mean crystallite size was calculated by the Scherrer method from the FWHM (full width at half maximum) of the (101) peak of TiO₂ anatase phase. The XRD measurements were carried out with the help of early stage researcher, Ibrahim Dündar.

3.8.2. Raman Spectroscopy

The Raman spectroscopy was used to further analyze the structural properties of TiO₂ thin films. Both as deposited and annealed TiO₂ thin films on glass and Si substrates were measured by Raman spectroscopy.

Raman spectra were acquired on a micro-Raman spectrometer HORIBA Jobin Yvon Model HR800 in the spectral range of 100-800 cm⁻¹ using 532 nm laser line which delivers 5 mW of power at 10 μm laser spot size during measurement. The Raman measurements were carried out with the help of early stage researcher, Ibrahim Dündar.

3.8.3. UV-visible spectroscopy

The total transmittance and total reflectance of TiO₂ thin films on glass substrates and total reflectance of TiO₂ thin films on Si substrates were measured by Jasco V-670 spectrophotometer with spectral range between 200 and 1200 nm. The optical properties of both as-deposited and annealed samples were investigated. The film thickness of TiO₂ thin films was calculated by spectra manager program using interference fringes from the spectrum of total transmittance and total reflectance. The optical measurements were carried out with the help of early stage researcher, Ibrahim Dündar.

3.8.4. Current-voltage measurements

Current-Voltage (I-V) measurement was performed to investigate the electrical properties of TiO₂ thin film on glass and Si substrates and the properties of TiO₂ hybrid solar cells. The Autolab PGSTAT 30 system was used for measuring of I-V curves of the films. The software Frequency response analyzer was used to obtain the data.

DC measurements were carried out for the TiO₂ thin films on glass substrates by using two graphite contacts with a distance of 5 mm on the top of TiO₂ thin film. However, AC measurements were

carried out for the TiO₂ thin films on Si substrates by using a graphite contact (d= 3.5 mm) and Si as a second contact. All samples were measured in dark to reduce the effect of light. The I-V measurements were carried out with the help of Senior Research Scientist, Arvo Mere.

The Current-Voltage (I-V) measurement was also performed for the TiO₂ hybrid solar cells. The TiO₂ hybrid solar cells were placed under simulated sunlight DC measurements were carried out to get the I-V curve. The out-put properties of the TiO₂ hybrid solar cells were characterized by recording the I-V curves under simulated sunlight (100 mW/cm²). This measurement was carried out with the help of Research Scientist, Atanas Katerski.

4. RESULTS AND DISCUSSIONS

4.1. Optical properties of TiO₂ thin films

4.1.1. Total Transmittance of TiO₂ thin films deposited onto glass substrates

The optical transmittance spectra of TiO₂ thin films deposited onto glass substrates at temperatures from 200 to 500 °C and followed by annealing at 500 °C are presented in Fig. 4.1. The transmittance of TiO₂ films are very high in the visible light range with the highest transmittance of 93% for the as-deposited sample (Fig. 4.1(a)) and 84% for the annealed sample (Fig. 4.1(a)). It can be seen that the spectra show more periodic interference fringes with increasing the deposition temperature from 200 to 500 °C indicating that the thickness of the film became higher [27].

Moreover, the total transmittance of as-deposited films decreased from 93% (Fig. 4.1(a)) to 83% (Fig. 4.1(d)) with increasing the deposition temperature from 200 to 500 °C. This phenomenon is because of the change of crystalline structure of the film according to XRD results (see section 4.2.1) and the increase of the film thickness [25].

The total transmittance also decreased after annealing. The interference patterns indicate the homogeneity of the films. The decrease in the optical transmittance after annealing can be related to the increase in surface roughness and enhance the light diffusion [27].

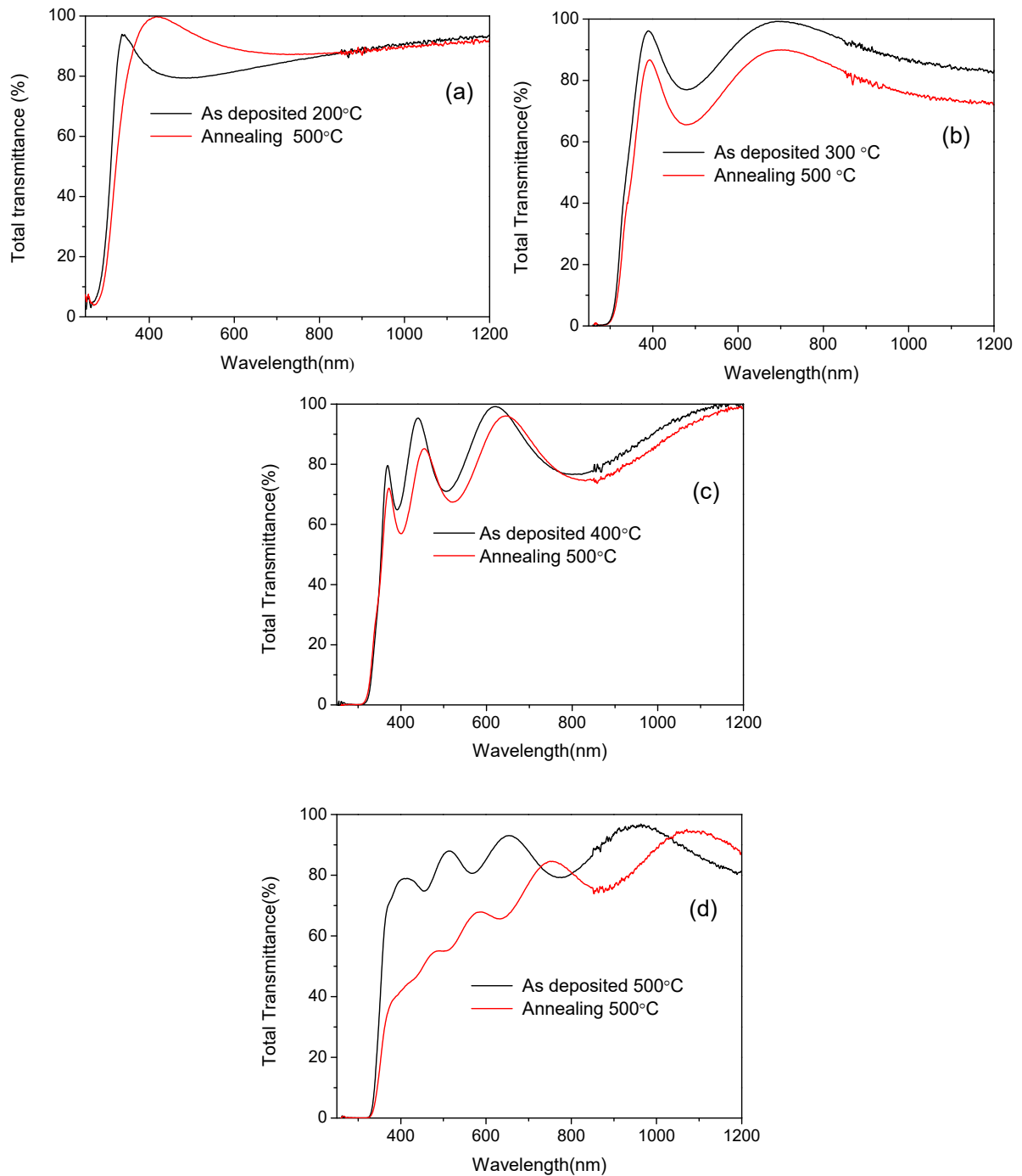


Figure 4.1 Total transmittance spectra of TiO₂ thin films deposited from 200 to 500 °C on glass substrates and followed by annealing at 500 °C. (a) as-deposited at 200 °C, (b) as-deposited at 300 °C, (c) as-deposited at 400 °C, (d) as-deposited at 500 °C.

4.1.2. Thicknesses of the TiO₂ thin films on glass and Si substrates

The thicknesses of TiO₂ thin films were determined by using interference fringes from optical spectrum. This method was first reported by Swanepoel [61].

The total transmittance was used for the thicknesses measurement of TiO₂ thin films on glass substrates. The total reflectance was selected for the thicknesses measurements of films on Si substrates. The peaks and valleys of the interference fringes at the transmittance and reflectance spectrum were spotted in Fig. 4.2.

The refractive index of TiO₂ in thin film was determined as 2.2. This value is from previous research in the laboratory of thin film technologies [26]. Then if the refractive index is known, the film thickness can be calculated using the following equation [62]:

$$d = \frac{p}{2\sqrt{n^2 - \sin^2 \theta}} \times \frac{\lambda_1 \times \lambda_2}{\lambda_1 - \lambda_2} \quad (4.1)$$

Where

d- film thickness, nm,

n- refractive index,

θ- the angle of incident light,

p- periodicity of interference wave between peak and valley,

λ₁- the wavelength of peaks, nm,

λ₂- the wavelength of valleys, nm.

In order to keep the stability and accuracy of the calculated value, the interference fringes were selected between pairs of adjacent peaks and valleys, except the ones near absorption range where transmittance starts to decrease.

For example, Fig. 4.2 (a) showed the transmittance of TiO₂ thin film on glass substrate which is deposited at 400 °C, two pairs of peaks and valleys were selected between the wavelength of 400 and 644 nm, other peaks and valleys were not selected. Similarly, the peaks and valleys were selected the same way for the films on Si substrates, one sample is shown in Fig. 4.2 (b). All other samples were calculated by this method, and the results were summarized in Table 4.1.

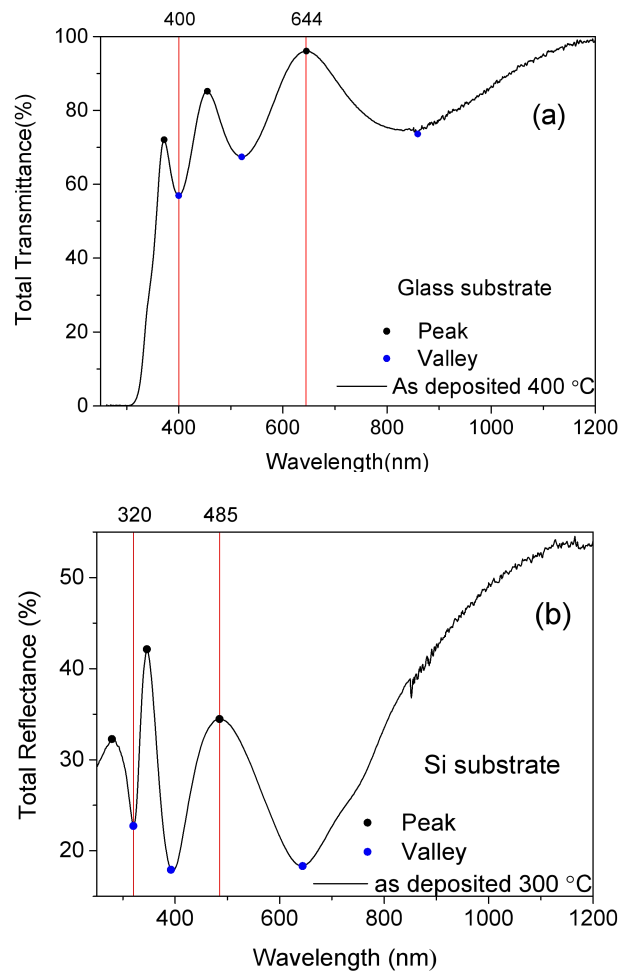


Figure 4.2 Total transmittance of TiO₂ thin film deposited at 400 °C on glass substrate (a) and Total reflectance TiO₂ thin film deposited at 400 °C on Si substrate (b).

The thicknesses for films on glass and Si substrates are presented in Table 4.1. It is found that the thickness increased with increasing the deposition temperature for both as deposited films on different substrates. The thicknesses of as-deposited films increased from 110 to 620 nm for films

deposited onto glass substrates and from 110 to 603 nm for films deposited onto Si substrates on increasing deposition temperature from 200 to 500 °C.

It is observed that the film thicknesses of films deposited onto Si substrates are slightly lower than the thickness of films deposited onto glass substrates. This is also reported in the ref [63]. The film thickness increases with the increase of deposition temperature were also observed in other chemical spray pyrolysis methods[22],[25]. Since the solution feed rate was consistent, then it is implicit that the film thickness increased with increasing deposition temperature owing to the increase in the growth rate. However, the film thickness decreased after annealing at 500 °C for films on glass and Si substrates compared to as-deposited films. This is related to the burning out of the organic residues in the film [26].

Further annealing at 700 °C led to thinner films on Si substrates compared to the films on Si substrates annealed at 500 °C.

Table 4.1 Film thickness of TiO₂ films on glass and Si substrates at various substrate temperatures (T_s) and annealing temperature.

T _s (°C)	Film thickness (nm)				
	Film on glass substrate		Film on Si substrate		
	As-deposited	Annealed at 500 °C	As-deposited	Annealed at 500 °C	Annealed at 700 °C
200	120	80	110	80	70
300	180	170	185	170	160
400	370	320	365	320	310
500	620	510	600	500	480

4.1.3. The band gap of TiO₂ thin films deposited onto glass substrates

The indirect optical band gap was calculated by using the optical transmittance and reflectance for TiO₂ thin films on glass substrates. To further characterize the optical properties of deposited TiO₂ films, the band gap was calculated using the Tauc relation [25]:

$$\alpha(h\nu) = B(h\nu - E_g)^m \quad (4.2)$$

where

α - the absorption coefficient,

$h\nu$ - the photon energy, eV,

E_g - the optical band gap, eV,

B- constant, which does not depend on the energy,

m- constant, which characterizes electronic conversion of light absorption. ($m=1/2$ for allowed direct transitions, $m=2$ for allowed indirect transitions).

The transmittance of the thin films is affected by both reflectivity and combination of absorption coefficient and film thickness. The equation (4.3) [64] is used to eliminate the effect of the interference fringes on the transmittance (T) and spectrum is shown in Fig. 4.3.

$$T/(1 - R) = e^{-\alpha d} \quad (4.3)$$

where

α - absorption coefficient,

d- film thickness, nm,

T- total transmittance,

R- total reflectance.

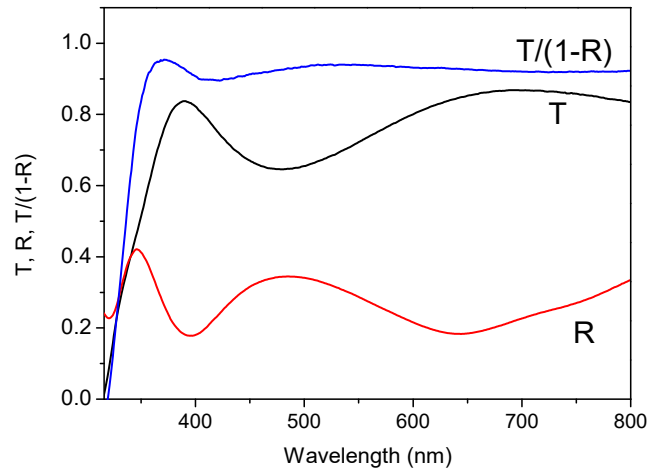


Figure 4.3 optical spectrum of T, R, $T/(1-R) = e^{-\alpha d}$ (T= transmittance, R= reflectance.)

The direct band gap was assumed for the films on glass substrates, so the equation two can be written as:

$$(\alpha \cdot hv)^2 = B^2 (hv - E_g) \quad (4.4)$$

The optical band gap was obtained by extrapolating the linear part of the plot of $(\alpha hv)^2$ against hv to the photon energy axis is shown in Fig. 4.4.

The band gaps of the as-deposited films were 3.5, 3.4, 3.4, 3.3 eV with increasing deposition temperature from 200 to 500 °C and it decreased slightly after annealing at 500 °C, giving the values of 3.5, 3.4, 3.3 and 3.2 eV, respectively. It is found that the band gap of as-deposited films decreased with increasing substrate temperature. This might be the result of the increased crystallinity of the annealed films [65].

The similar value of band gap was observed by other researchers. The most observed band gap value is in the range of 3.5-3.2 eV [23-25]. Nakaruk *et al.* [27] studied TiO₂ films deposited onto quartz substrates at 400 °C by ultrasonic spray pyrolysis method and annealed at 600 °C, 800 °C, 1000 °C show the indirect band gap decreased from 3.54 eV to 3.26 eV. Lin *et al* [65] has reported the optical

indirect band gap of the crystalline TiO₂ films by spin coating method decreased slightly from 3.5 eV to 3.4 eV with increasing annealing temperatures from 300 to 500 °C.

Annealing at a higher temperature will remove organic residuals and enhance the quality of crystallinity which also affects the band gap value [27].

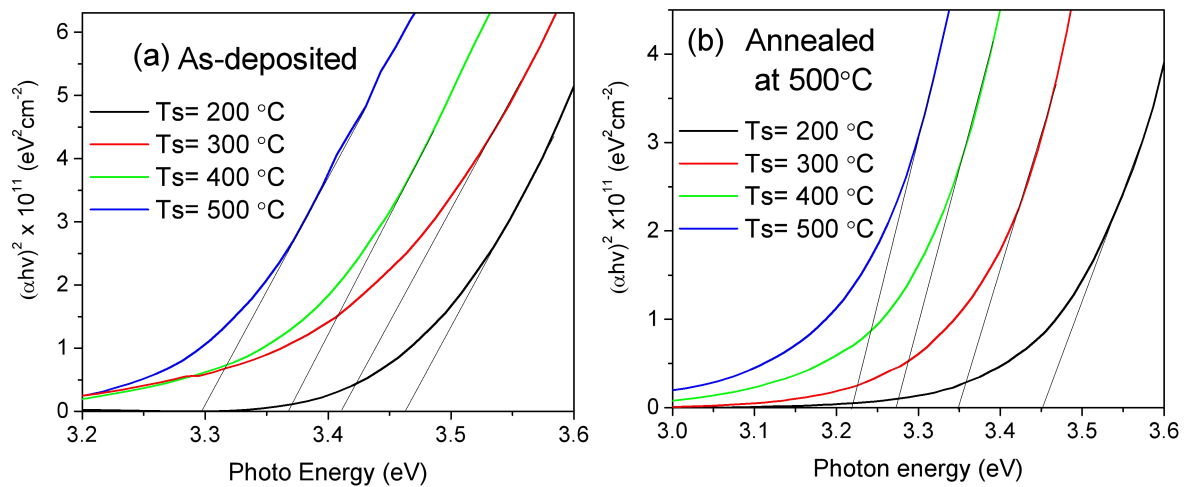


Figure 4.4 Band gap of TiO₂ thin films on glass substrates: (a) as-deposited films deposited at substrate temperature from 200 to 500 °C. (b) as-deposited films followed by annealing at 500 °C.

4.2. Structural properties of TiO₂ thin films

4.2.1. XRD results of TiO₂ thin films deposited on glass substrates

Fig. 4.5 shows the XRD result of TiO₂ thin films on glass substrates deposited at different deposition temperatures from 200 to 500 °C and annealed at 500 °C. XRD studies show that the as-deposited films prepared at substrate temperatures below 500 °C are amorphous. The diffraction peaks at 25.3°, 37.7°, 48.1°, 53.9° and 55.1° correspond to the (101), (004), (200), (105) and (211) planes of anatase phase [66].

The (101) anatase diffraction peak becomes apparent with poor crystallinity for the films deposited at 500 °C (Fig. 4.5(a)). Annealing at 500 °C results in anatase phase for films deposited at or above 300 °C (Fig. 4.5(b)). The intensity of anatase peak (101) has gradually increased for the films

deposited from 300 °C to 500 °C after annealing at 500 °C (Fig 4.5(b)). No rutile peaks were detected due to relatively low annealing temperature. It is also observed that the intensity of anatase peak (101) for film deposited at 500 °C has significantly increased after annealing at 500 °C which is related to the improvement of the quality and purity of crystallinity [67].

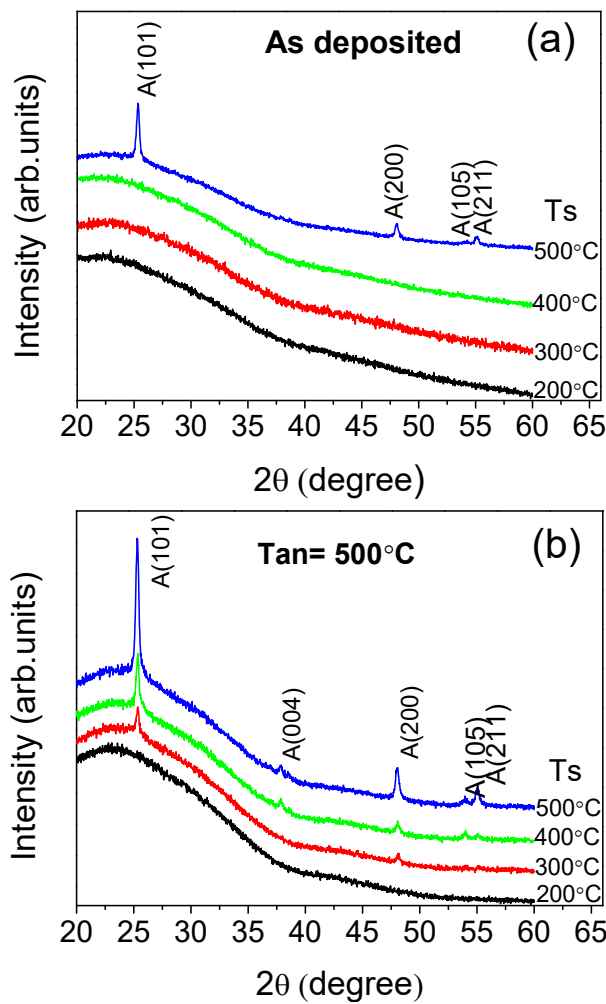


Figure 4.5 XRD patterns of TiO₂ thin films on glass substrates deposited at various temperatures from 200 to 500 °C: (a) as-deposited thin films, (b) thin films annealed at 500 °C. (A-Anatase)

4.2.2. XRD results of TiO₂ thin films deposited on Si substrates

Fig. 4.6 shows the XRD results of TiO₂ thin films on glass substrates deposited at 200 to 500 °C and annealed at 500 °C and 700 °C.

XRD result showed that the films deposited at or below 300 °C are amorphous. However, the films deposited at or above 400°C have a very poor crystallinity structure of anatase phase. Annealing at 500°C results in the formation of anatase phase regardless of the deposition temperature. The film deposited at 500 °C and followed by annealing at 500 °C shows diffraction peaks of anatase phase at 2θ values of 25.4, 37.8, 48.1, 55.2, 53.8 which correspond to the planes of (101), (004), (200), (105) and (211), respectively. The diffraction peak at $2\theta = 33.6^\circ$ belongs to the Si substrate [68].

Further annealing at 700 °C has significantly changed the film crystalline structure, a mixed anatase-rutile phase is observed and the peak at $2\theta=27.4^\circ$ belongs to rutile structure [69]. The films deposited below or at 400 °C remain anatase. However, the films deposited at 500 °C composed of the mixture of anatase and rutile phases.

It is considered pure bulk anatase phase starts to transform irreversibly to rutile phase at 600 °C in air [70]. However, the temperature for the transformation of anatase to rutile phase has been reported to vary between 600 °C and 1200 °C [26,27] due to the use of different methods, precursors and deposition temperature.

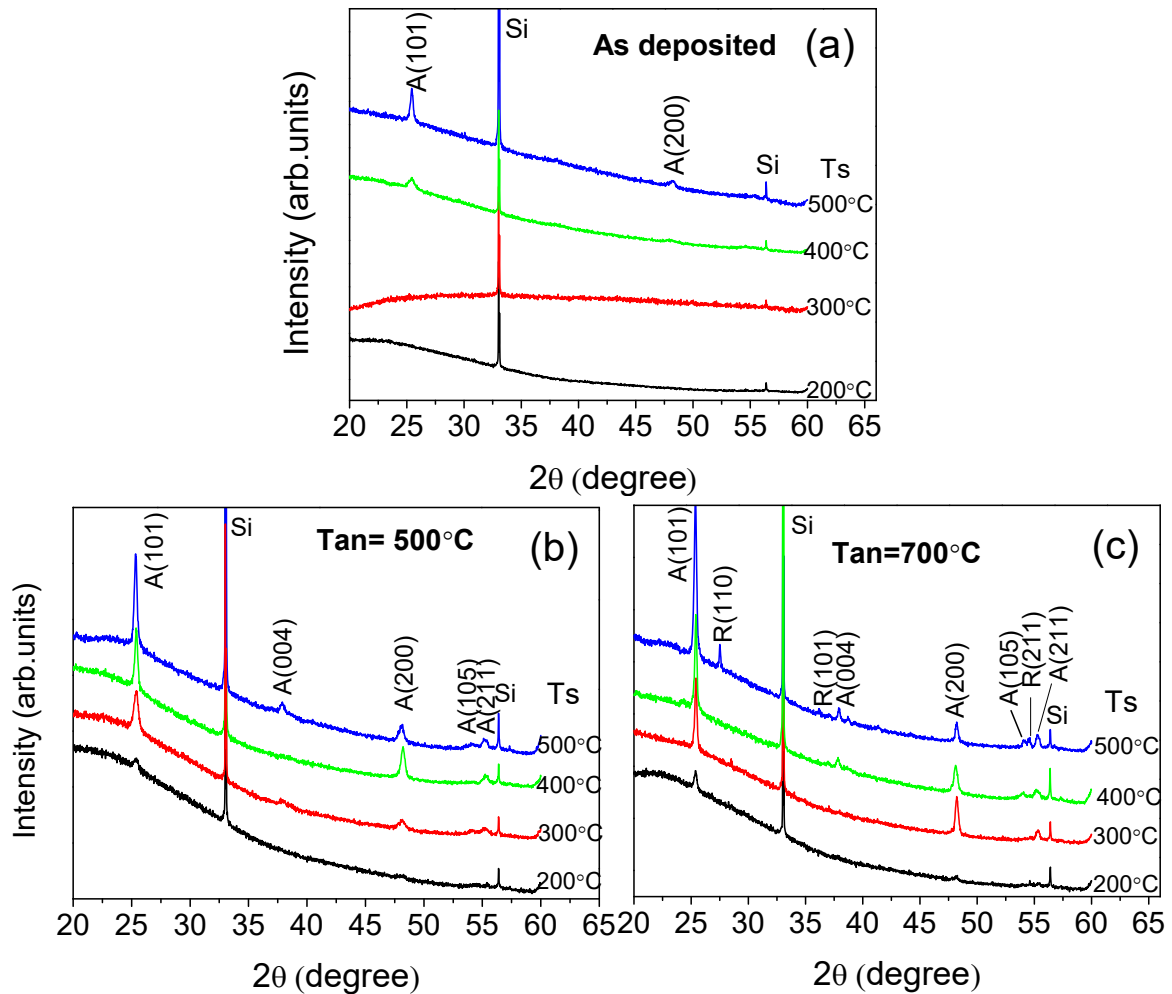


Figure 4.6 XRD patterns of TiO₂ thin films on silicon substrates. (a) as-deposited thin films, (b) thin films annealed at 500 °C, (c) thin films annealed at 700 °C. (Si means Si-substrate, A- anatase, R- rutile).

The mean crystallite size of the TiO₂ films deposited onto different substrates and annealed at different temperatures were calculated by applying the Scherrer's formula [26]. The equation is below:

$$d = \frac{k\lambda}{\beta \cos \theta} \quad (4.5)$$

Where

d- crystallite size, nm,

k- shape constant, 0.9,

λ - X-ray wavelength of Cu-k α radiation, nm,

θ - Bragg's angle in degrees,

β -the FWHM in radians.

The anatase (101) peak was selected for estimating the average crystallite size for films on glass and Si substrates, the values obtained are presented in Table 4.2.

It showed that the mean crystallite size of anatase phase increased with increasing deposition temperature and annealing temperature.

The mean crystallite size of TiO₂ films deposited in the temperature range of 300 to 500°C and annealed at 500°C varies from 26 to 32 nm. The mean crystallite size of anatase phase has been reported in the literature to vary in the range of 21-38 nm [20,27].

Moreover, further annealing at 700 °C enhanced the crystallinity of films deposited onto Si substrates. Annealing of TiO₂ thin films can increase the mean crystal size [65].

From the Table 4.2, we can see the mean crystallite size of TiO₂ films deposited onto Si substrates is slightly larger than onto glass substrates. This indicates that substrates have a significant influence on the crystal structure of TiO₂ thin films [71,72].

Table 4.2 The mean crystallite size of TiO₂ thin films deposited at different deposition temperature (T_s) and annealed at 500 °C and 700 °C.

Deposition temperature T _s (°C)	Mean crystallite size (nm)				
	Glass substrate		Silicon substrate		
	As-deposited	Annealed at 500 °C	As-deposited	Annealed at 500 °C	Annealed at 700 °C
200	-	-	-	21	30
300	-	26	-	28	37
400	-	29	17	31	40
500	28	32	31	32	42

XRD results show that crystalline TiO₂ films with anatase structure occur at 400 °C if films are deposited at Si substrate and at 500 °C if films are deposited on glass substrate. This is because the temperature from the substrates is different, the thermal conductivity of Si is higher than glass. So the temperature from Si substrate is higher than from glass substrate even at the same deposition temperature.

According to the literature, the substrate used may influence the films growth, due to the nature of the substrate, crystalline or amorphous, provides different degrees of packing and, consequently, different stages of density and thickness in the morphological structure of the obtained films. It is also attributed to the mobility of the atoms on the substrate surface which is responsible for the degree and type of nucleation on the substrate [73].

4.2.3. Raman results of TiO₂ thin films deposited on glass substrates

Raman spectrum was used to confirm the crystal structure of TiO₂ films. Fig. 4.7 shows Raman spectra of TiO₂ films grown at different substrate temperature and annealed at 500 °C. TiO₂ thin films grown onto glass substrates (Fig. 4.7(a)) exhibit the bands at around 142 (E_g), 197 (E_g), 398 (B_{1g}), 520 (B_{1g}) and 639 (E_g) cm⁻¹ which are assigned to TiO₂ anatase [74]. For anatase phase the values of 142 cm⁻¹, 197 cm⁻¹ and 398 cm⁻¹ are attributed to vibrations of O-Ti-O and the values of 520 cm⁻¹ and 639 cm⁻¹ belong to vibrations of Ti-O [75].

No rutile peaks were detected after annealing at 500 °C. The results are in agreement with XRD.

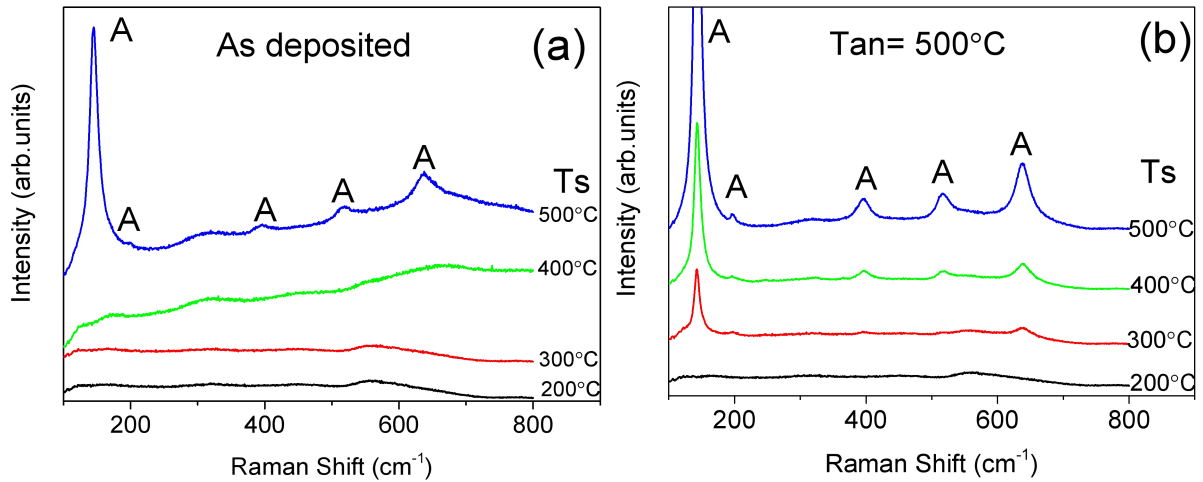


Figure 4.7 Raman spectrum of TiO₂ thin films on Si substrates. (a) films deposited at 200 °C, 300 °C, 400 °C, 500 °C, (b) films annealed at 500 °C. (A - anatase)

4.2.4. Raman results of TiO₂ thin films deposited on Si substrates

Fig. 4.8 shows the TiO₂ thin films deposited on silicon substrates and annealed at 500 °C, 700 °C. The as deposited film (Fig. 4.8(a)) grown at 400 °C-500 °C showed anatase peaks at 144, 197, 398 and 635 cm⁻¹, the additional peaks at 302 and 520 cm⁻¹ belong to the Si substrate [76].

After annealing at 500 °C (Fig. 4.8(a)) and 700 °C (Fig. 4.8(c)), the films showed anatase phase if deposited in the temperature of 200 to 500 °C.

Moreover, TiO₂ films deposited at 500 °C and annealed at 700 °C showed additional Raman bands at round 232 (B_{1g}) and 440 (E_g) cm⁻¹ which belong to rutile phase [76], and thereby confirm a mixture of anatase and rutile phases in these films. This suggests annealing at higher temperature will transform anatase to rutile phase. The mixture phases after annealing above 700 °C have also been observed in sol-gel spin coating and ultrasonic spray pyrolysis [26,27].

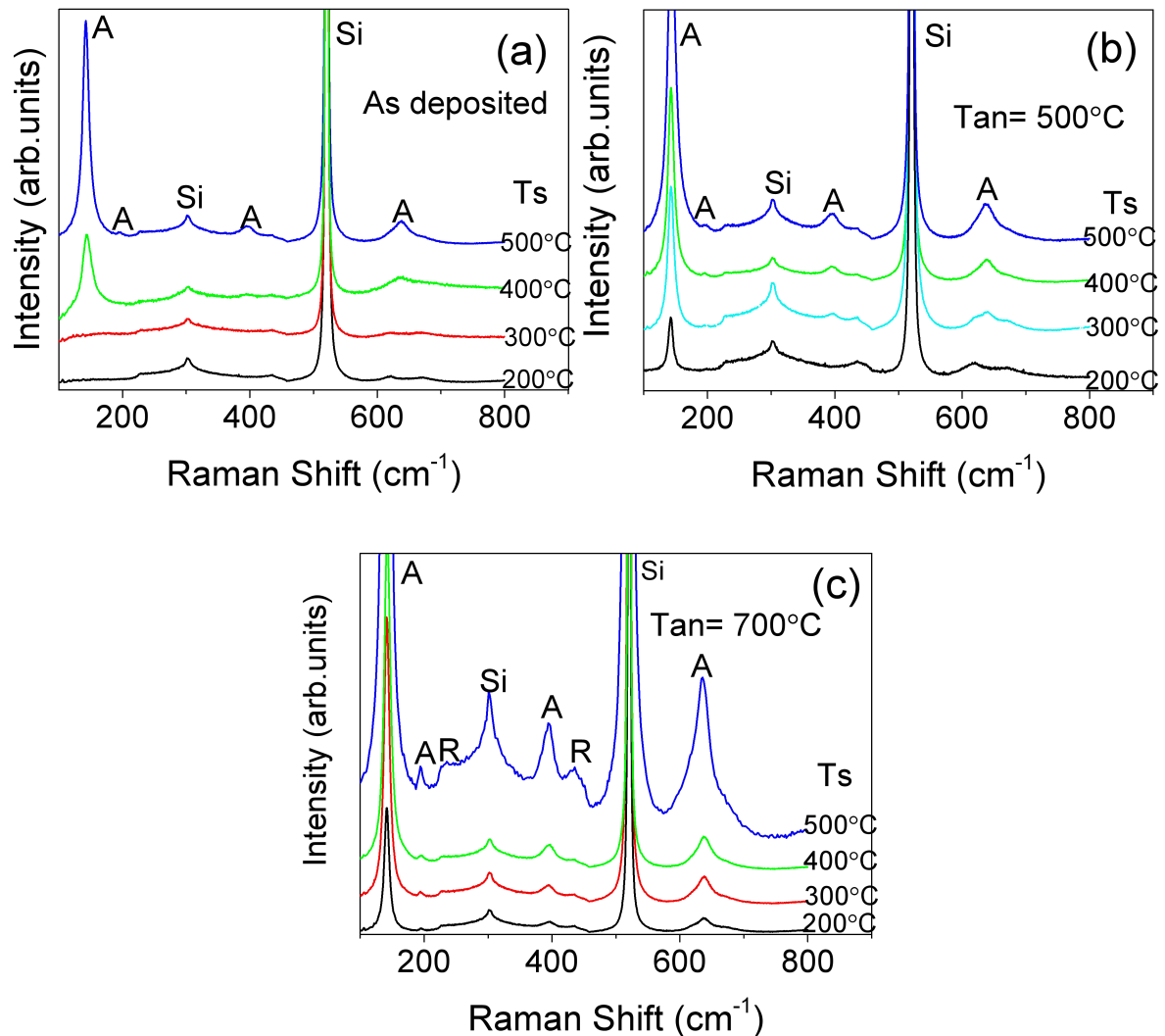


Figure 4.8 Raman spectrum of TiO₂ films deposited Si substrates: (a) films deposited at 200 °C, 300 °C, 400 °C, 500 °C, (b) films annealed at 500 °C, (c) films annealed at 700 °C. (Si means Si-substrate, A- anatase, R- rutile)

To summarize, the Raman results indicated the films on glass substrates showed anatase phase when deposited at 500 °C, but 400 °C for films on Si substrates. After annealing at 500 °C, all films turned to anatase phase regardless of deposition temperature except the film on glass substrate deposited at 200 °C was still amorphous. Further annealing at 700 °C for the film on Si substrate deposited at 500 °C showed rutile phase. Raman study corresponds to XRD results.

4.3. Electrical properties of TiO₂ thin films

4.3.1. The electrical resistivity of TiO₂ thin films deposited on glass substrates

The electrical resistivity of TiO₂ thin films deposited on glass substrates were measured by applying two graphite contacts with a distance (L= 5 mm) on the top of TiO₂ film as shown in Fig. 4.9.



Figure 4.9 one example of I-V measurement of film on glass substrate

The electrical resistivity was measured in dark at room temperature. The value of resistivity can be obtained from the equation below:

$$\rho = \frac{V}{I} \cdot \frac{D \cdot W}{L} \quad (4.6)$$

Where

ρ - resistivity, $\Omega \cdot \text{cm}$,

V-Voltage,V,

I- current,A,

D- TiO₂ film thickness,cm,

W- the width of the film in measured range, cm,

L- distance between contacts,cm.

The electrical resistivity of TiO₂ thin films on glass substrates is presented in Fig. 4.10. It can be seen that the resistivity decreased with increasing the deposition temperature. It is related to the fact that

by increasing the deposition temperature the quality of crystallite structure become better and the film thickness is increasing [77]. The resistivity value is in a range of 10^5 - $10^6 \Omega \cdot \text{cm}$ which is similar to the values reported by other researchers [72,78]. Annealing at 500 °C led to the decrease of resistivity in all deposited samples. The decrease in resistivity after annealing is due to the grain size increases after annealing which leads to a decrease in grain boundaries and hence resistivity [78]. Larger grain size will provide higher surface contact between the TiO_2 film and the electrode, thereby improving electron migration.

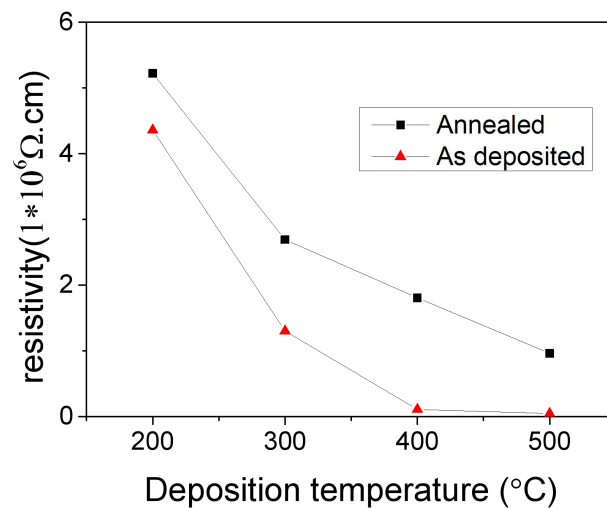


Figure 4.10 Resistivity of TiO_2 thin films on glass substrates deposited at 200 °C, 300 °C, 400 °C, 500 °C and annealed at 500 °C.

4.3.2. Electrical resistivity of TiO_2 thin films deposited on Si substrates

The electrical resistivity of TiO_2 thin films deposited on Si substrates were measured by applying two graphite contacts, one contact is on the top of TiO_2 thin film, another contact is connected to the Si substrate (Fig. 4.11).

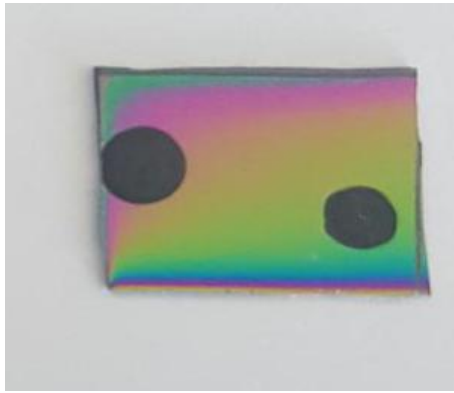


Figure 4.11 One example of resistivity measurement of TiO₂ on Si substrate

The electrical resistivity was also measured in dark at room temperature. The equation used for calculation of resistivity is different from the one used for film on glass substrate:

$$\rho = \frac{V}{I} \cdot \frac{\pi \cdot D^2}{4T} \quad (4.7)$$

Where

ρ - resistivity, $\Omega \cdot \text{cm}$,

V-Voltage, V,

I- current, A,

T- TiO₂ film thickness, cm,

D- diameter of the graphite contact on the top of TiO₂ film, cm.

The resistivity of the films decreases with increasing deposition temperature from 200 to 300 °C, which may be due to the change of crystal structure from amorphous to crystalline anatase phase. This result is coincident with the result measured from films on glass substrates. However, the resistivity value of films on Si substrates is in the range of 10^2 - $10^4 \Omega \cdot \text{cm}$ which is much smaller than the value measured on films on glass substrates. This phenomenon is also observed by another researcher [72]. The resistivity also decreased when increasing the annealing temperature; this

phenomenon is due to increase in the grain size which leads to a decrease in the grain boundaries and hence resistivity [65].

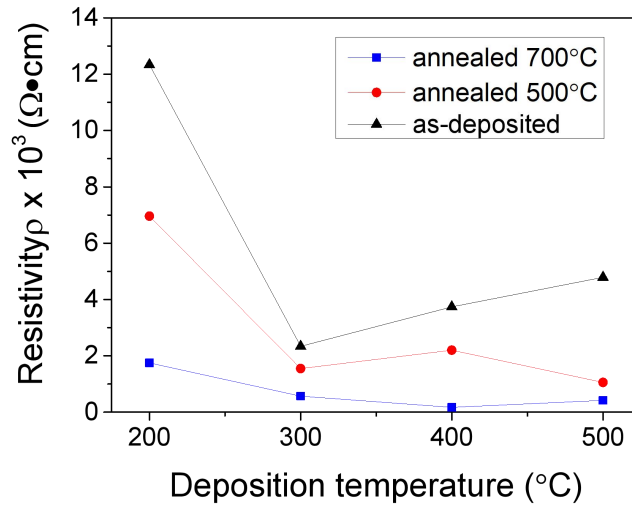


Figure 4.12 Resistivity of TiO₂ films deposited on silicon substrates at various substrate temperatures (T_s) and after various annealing temperatures

The calculated resistivity of TiO₂ films on Si substrates is much lower than the resistivity of TiO₂ films on glass substrates. This is related to the different I-V measurements of TiO₂ films. The difference could be also from the substrates, as Si is semiconductor, it has much lower resistivity than glass (insulator), which can provide much more free charge carriers to increase the mobility of electrons in TiO₂ thin film hence reduce the resistivity.

4.4. Solar cell properties

TiO₂ thin films deposited at 300 °C and 400 °C, indicating lowest resistivity, were tested in a solar cell with structure of glass /ITO/TiO₂/P3HT/Au. In this structure, ITO is front contact, TiO₂ is window layer, P3HT is hole conductor and Au is back contact. The test solar cell structure did not consist of an absorber layer. The fabricated solar cell is shown in Fig. 4.13.



Figure 4.13 One example of tested solar cell

The performance of the solar cell was examined using a solar simulator at an intensity of 100 mW/cm². The fill factor and conversion efficiency of the cells were characterized by the following equations[79]:

$$FF = \frac{I_{\max} \times V_{\max}}{I_{sc} \times V_{oc}} \quad (4.8)$$

Where

I_{\max} - maximum output of current,A,

V_{\max} - maximum output of voltage, V,

I_{sc} - short-circuit current, A,

V_{oc} - open-circuit voltage, V.

The total energy conversion efficiency was defined as follows:

$$\eta = \frac{I_{sc} \times V_{oc} \times FF}{P_{in}} \quad (4.9)$$

Where

I_{sc} - short-circuit current, A,

V_{oc} - open-circuit voltage, V,

FF- fill factor,

P_{in} - intensity of the incident light, w.

Fig. 4.14 shows the I-V curves of TiO₂ solar cells with different deposition temperature. The parameters of the performances of TiO₂ solar cells are as summarized in Table 4.3. The I-V measurements were performed under the illumination intensity of 100 mw/cm², it can be seen from Table 4.3 that the out-put characteristics of the open circuit voltage (V_{oc}) improved from 390 mV to 460 mV when deposition temperature of TiO₂ thin films increased from 300 to 400 °C and followed by annealing at 500 °C. The open circuit current is very low because of the lack of an absorber layer. The increase of V_{oc} might be related with the facts that the band gap of TiO₂ decreases with increasing the deposition temperature, and this contributes to the ability of TiO₂ to absorb more light[74]. Surface area will be also increased with the increase by deposition temperature, due to the formation of more crystalline material, which will enhance light absorption [66].

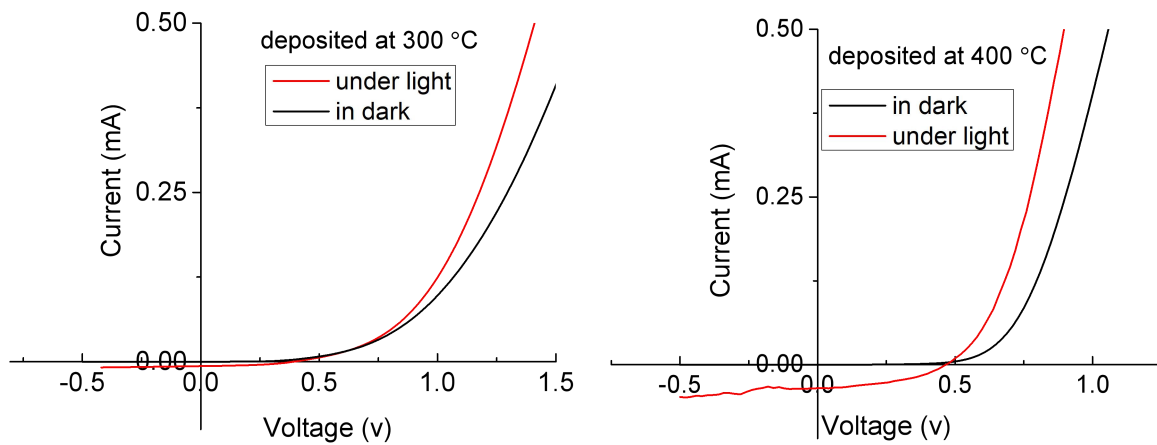


Figure 4.14 The I-V characteristics of solar cell structure glass/ITO/TiO₂/P3HT/Au, where TiO₂ thin films are deposited by ultrasonic spray pyrolysis at 300 °C (figure left) and 400 °C (figure right) and followed by annealing at 500 °C

Table 4.3 Out-put parameters of solar cell structure glass/ITO/TiO₂/P3HT/Au where TiO₂ thin films are deposited by ultrasonic spray pyrolysis at 300 °C (figure left) and 400 °C (figure right) and followed by annealing at 500 °C

TiO₂ solar cells	V_{oc} (mV)	J_{sc} (mA/cm²)	FF (%)	Efficiency (%)
(a) As deposited at 300 °C, followed by annealing at 500 °C	390	0.09	44	0.02
(b) As deposited at 400 °C, followed by annealing at 500 °C	460	0.15	46	0.03

5. SUMMARY

TiO₂ thin films were deposited onto glass, Si and ITO coated glass substrates by ultrasonic spray pyrolysis method. The effect of deposition and annealing temperature on the structural, optical, electrical properties and the performance of TiO₂ thin films in solar cell with structure of glass/ITO/TiO₂/P3HT/Au were investigated.

The conclusions are summarized below:

(1) The XRD data reveals that the as-deposited TiO₂ films grown below 400 °C onto glass substrate and below 300°C onto Si substrate are amorphous. Annealing at 500 °C results in formation of anatase structure if the films are deposited at temperatures ≥ 300 °C onto glass substrates or in the temperature range of 200-500 °C onto Si substrates. The mean crystallite size of anatase structure remains in the range of 20-32 nm irrespective of the deposition, annealing temperature and substrate. Further annealing of TiO₂ films on Si substrate at 700 °C led to the formation of the mixture of anatase and rutile phase if deposited at 500 °C and increase in the average crystallite size of the anatase structure to the range of 30-40 nm.

(2) According to the optical properties of TiO₂ films, the as-deposited TiO₂ films show high optical transmittance and band gap values in the range of 3.5-3.3 eV if deposited in the temperature range of 200-500 °C. Band gap and optical transmittance of TiO₂ thin films were found to decrease after annealing at 500 °C. Film thickness was found to increase with deposition temperature and decrease after annealing at 500 °C. The thicknesses of as-deposited films increased from 110 to 620 nm for films deposited onto glass substrates and from 110 to 603 nm for films deposited onto Si substrates with increasing deposition temperature from 200 to 500 °C. The film thicknesses of films deposited onto Si substrates are slightly smaller than the thickness of films deposited onto glass substrates.

(3) The resistivity of TiO₂ films depends on the deposition temperature and was found to decrease with increasing the annealing temperature. The resistivity value of films on Si substrates are in the range of 10^2 - 10^4 Ω ·cm. The resistivity of the films on glass substrates are the range of 10^5 - 10^6 Ω ·cm.

(4) TiO₂ thin films were tested in a solar cell device with a structure of glass/ITO/TiO₂/P3HT/Au. The results of the fabricated solar cells with a structure of glass/ITO/TiO₂/P3HT/Au showed better

performance if TiO₂ thin films were deposited at 400 °C rather than 300 °C and followed by annealing at 500 °C. Most probably this is related with higher V_{oc} value recorded at 460 mV for 400 °C deposited TiO₂ film than 390 mV if TiO₂ films were deposited at 300 °C. This finding suggest that TiO₂ films deposited at 400 °C and annealed at 500 °C are in favor in the case of solar cell applications.

The results of the thesis were presented as oral presentation at CYSENI 2018 conference and published in proceedings of ISSN 1822-7554.

5. ACKNOWLEDGEMENTS

This study was financially supported by the Estonian Ministry of Education and Research project IUT19-4, and by the European Union through the European Regional Development Fund project TK141 “Advanced materials and high-technology devices for energy recuperation systems”.

6. LIST OF REFERENCES

- [1] AJ Cavallo. Hubbert's petroleum production model: an evaluation and implications for World Oil Production Forecasts. *Nat Resour Res*, 2004; vol. 13.
- [2] I Ganesh, PP Kumar, I Annapoorna, JM Sumliner, M Ramakrishna, NI Hebalkar. Preparation and characterization of Cu-doped TiO₂ materials for electrochemical, photoelectrochemical, and photocatalytic applications. *Appl Surf Sci*, 2014, vol. 293, p. 229-247.
- [3] MaltiGoel. Solar rooftop in India: Policies, challenges and outlook. *Green Energy & Environment*. 2016, vol. 1, p. 129-137.
- [4] QL Ma, SQ Ma, YM Huang. Enhanced photovoltaic performance of dye sensitized solar cell with ZnO nanohoneycombs decorated TiO₂ photoanode. *Materials letters*, 2018, Vol. 218, p. 237-240.
- [5] M Lira-Cantu, A Chafiq, J Faissat, I Gonzalez-Valls, YH Yu. Oxide/polymer interfaces for hybrid and organic solar cells: Anatase vs. Rutile TiO₂. *Solar energy materials and solar cells*, 2011, Vol.95, p.1362-1374.
- [6] E Nouri, MR Mohammadi, ZX Xu, V Dracopoulos, P Lianos. Improvement of the photovoltaic parameters of perovskite solar cells using a reduced-graphene-oxide-modified titania layer and soluble copper phthalocyanine as a hole transporter. *Physical chemistry chemical physics*, 2018, Vol, 20, p. 2388-2395.
- [7] T Ivanova, A Harizanova, T Koutzarova, B Vertruyen. Characterization of nanostructured TiO₂: Ag films: structural and optical properties. *Journal of Physics Conference Series*, 2016, vol. 764, p. 12-19.
- [8] S Mahalingam, MJ Edirisinghe. Characteristics of electrohydrodynamically prepared titanium dioxide films. *Applied physics a-materials science & processing*, 2007, Vol. 89, p. 987-993.
- [9] S Paul, A Choudhury. Investigation of the optical property and photocatalytic activity of mixed phase nanocrystalline titania. *Applied nanoscience*, 2014, Vol. 4, p.839-847.

- [10] R Tobit, IG Esch. B Thomas. Surface structures and thermodynamics of low-index of rutile, brookite and anatase – A comparative DFT study. *Applied Surface Science*, 2014, vol.288, p.275–287
- [11] M Miyauchi, H Tokudome. Super-hydrophilic and transparent thin films of TiO₂ nanotube arrays by a hydrothermal reaction. *J Mater Chem* 2007; vol. 17, p. 2095–2100.
- [12] Y Sun, A Li, M Qi, L Zhang, X Yao. High surface area anatase titania nanoparticles prepared by MOCVD. *Mater Sci Eng B*, 2001, p. 185–188.
- [13] A. Nakaruk, G. Kavei, C.C. Sorrell. Synthesis of mixed-phase titania films by low-temperature ultrasonic spray pyrolysis. *Materials Letters*, 2010, vol. 64, p. 1365–1368.
- [14] Y Bai, MS Ivan, DA Filippo, B Juan, P Wang. Titanium Dioxide Nanomaterials for Photovoltaic Applications. *Chemical reviews*, 2014, Vol. 114, p. 10095-10130.
- [15] D Perednis, LJ Gauckler. Thin Film Deposition Using Spray Pyrolysis. *Journal of Electroceramics*, 2005, vol. 14, p. 103–111.
- [16] V Zharvan, R Daniyati, Nur Ichzan A. S., Gatut Yudoyono, Darminto. Study on fabrication of TiO₂ thin films by spin-coating and their optical properties. *AIP Conference Proceedings*, 2016, vol. 1719.
- [17] I Senain, N Nayan, H Saim. Structural and Electrical Properties of TiO₂ Thin Film Derived from Sol-gel Method using Titanium (IV) Butoxide. *Intergrated engineering*, 2010, vol. 2.
- [18] MB Tahir, S Hajra, M Rizwan, M Rafique. Optical, microstructural and electrical studies on sol gel derived TiO₂ thin films. *Indian Journal of Pure & Applied Physics*, 2017, Vol. 55, p. 81-85.
- [19] I. Karabay, S. Aydın Yüksel, F. Ongül, S. Öztürk, M. Asli. Structural and Optical Characterization of TiO₂ Thin Films Prepared by Sol–Gel Process. *Applied Physics and Materials Science*, 2012, Vol. 121.
- [20] AS Bakri, MZ Sahdan, F Adriyanto, NA Raship, NDM Said, SA Abdullah, MS Rahim. Effect of Annealing Temperature of Titanium Dioxide Thin Films on Structural and Electrical Properties. *AIP Conference Proceedings*, 2017, vol. 1788.

- [21] I Vaiciulis, M Girtan, A Stanculescu, L leontie, F Habelhames, S Antohe. on titanium oxide spray deposited thin films for solar cells applications. Proceedings of the romanian academy, Vol.13, p. 335–342.
- [22] A. Conde-Gallardo, M. Guerrero, N. Castillo, AB Soto, R Fragoso, JG Caban. TiO₂ anatase thin films deposited by spray pyrolysis of an aerosol of titanium diisopropoxide. Thin Solid Films, 2005, vol. 473, p.68–73.
- [23] S Sali, S Kermadi, L Zougar, B Benzaoui. Nanocrystalline proprieties of TiO₂ thin film deposited by ultrasonic spray pulverization as an anti-reflection coating for solar cells applications. Journal of Electrical Engineering, 2017, Vol. 68, p. 24–30.
- [24] R. Ayouchi, C. Casteleiro, R. Schwarz, J. R. Barrado, and F. Martín. Optical properties of TiO₂ thin films prepared by chemical spray pyrolysis from aqueous solutions. Physica status solidi c - current topics in solid state physics, 2010, vol. 7, p. 933– 936.
- [25] E Houda, M Boujnah, A Taleb. Thickness effect on the optical properties of TiO₂-anatase thin films prepared by ultrasonic spray pyrolysis: Experimental and ab initio study. International journal of hydrogen energy, 2017, Vol.42, p. 19467-19480.
- [26] I Oja, A Mere, M Krunk, R Nisumaa, CH Solterbeck, M Es-Souni. Structural and electrical characterization of TiO₂ films grown by spray pyrolysis. Thin Solid Films, 2006, vol. 515, p. 674-677.
- [27] A Nakaruk, D Ragazzon, CC Sorrell. Anatase-rutile transformation through high-temperature annealing of titania films produced by ultrasonic spray pyrolysis. Thin solid films, 2010, Vol. 518, p. 3735-3742.
- [28] D. Zhao, T. Peng, L. Lu, P. Cai, P. Jiang, Z. Bian, Effect of annealing temperature on the photoelectrochemical properties of dye-sensitized solar cells made with mesoporous TiO₂ nanoparticles. J. Phys. Chem. C, 2008, Vol. 112, p. 8486.
- [29] H. Hosono, K. Nomura, Y. Ogo, T. Uruga, T. Kamiya. Factors controlling electron transport properties in transparent amorphous oxide semiconductors. J. Non-Cryst. Solids, 2008, Vol.354, p. 2796.

- [30] S. Nakade, Y. Saito, W. Kubo, T. Kitamura, Y. Wada, S. Yanagida, Influence of TiO₂ nanoparticle size on electron diffusion and recombination in dye-sensitized TiO₂ solar cells, *J. Phys. Chem. B* 2003, Vol. 107, p. 8607.
- [31] JB Mooney, SB Radding. Spray pyrolysis processing. *Annual Review of Materials Science*, Volume: 12, Pages: 81-101.
- [32] P Dainius, G Ludwig. Deposition Using Spray Pyrolysis. *Journal of Electroceramics*, 2005, vol. 14, p. 103–111.
- [33] SS Yogesh, RT Nilesh, U Ashok. Influence of quantity of spray solution on the physical properties of spray deposited nanocrystalline MgSe thin films. *Physics and Mathematics*, 2016, vol. 2, p. 17-26.
- [34] Perednis, Dainius. Gauckler, Ludwig J. Thin Film Deposition Using Spray Pyrolysis. *Journal of Electroceramics*, 2005 vol. 14, p. 103–111.
- [35] NT Jitendra, NT Rajanish, SK Kwang. Zero-dimensional, one-dimensional, two-dimensional and three-dimensional nanostructured materials for advanced electrochemical energy devices. *Materials Science*, 2012, vol. 57, p. 724–803.
- [36] R. Suresh, V. Ponnuswamy, R. Mariappan. Effect of solvent and substrate temperature on morphology of cerium oxide thin films by simple nebuliser spray pyrolysis technique. *Materials Technology*, 2015, Vol.30, p. 11-22.
- [37] L Filipovic, M Ianeng, S Selberherr, GC Mutinati, E Brunet, S Steinhauer, A Köck, J Teva, J Kraft, J Siegert, F Schrank. Modeling Spray Pyrolysis Deposition, *Proceedings of the World Congress on Engineering*, 2013, Vol.2.
- [38] H.L. Tuller. Oxygen ion and mixed conductors and their technological applications. Boston: Kluwer Academic Publishers, 2000, Vol. 13, P79-87.
- [39] MS. Tomar, FJ Garcia. Spray pyrolysis in solar cells and gas sensors. *Crystal Growth Characterization*, 1981, Vol. 4, p. 221–248.

- [40] G. Cao. Nanostructures and nanomaterials: synthesis, properties and applications. London: Imperial College Press, 2004. Vol. 451, p.26.
- [41] HL Tuller. Oxygen ion and mixed conductors and their technological applications. Boston: Kluwer Academic Publishers, 2000, Vol. 473 p.27.
- [42] S Pramod. Patil. Versatility of chemical spray pyrolysis technique. Materials Chemistry and Physics, 1999, vol. 59, p. 185-198.
- [43] MF García-Sánchez, J Peña, A Ortiz, G Santana. Nanostructured YSZ thin films for solid oxide fuel cells deposited by ultrasonic spray pyrolysis. Solid State Ionics, Vol,179, 2008, P. 243-249.
- [44] SC Tsai, YL Song, CS Tsai. Ultrasonic spray pyrolysis for nanoparticles synthesis. Journal of Materials Science, 2004, vol. 39 p. 3647 – 3657.
- [45] S Kohtani, A Kawashima, H Miyabe. Reactivity of Trapped and Accumulated Electrons in Titanium Dioxide Photocatalysis. Catalysts, 2017, Vol. 7.
- [46] DF Rodriguez, PM Perillo, MP Barrera. High performance TiO₂ nanotubes antireflection coating. Materials science in semiconductor processing, 2017, Vol.71, p.427-432.
- [47] S Singh, V Sharma, K Sachdev. Investigation of post annealing effects on Nb: TiO₂ transparent conducting thin films. Advanced science letters, 2016, Vol. 22, p. 3773-3776.
- [48] T Ali, A Ahmed, MN Siddique, P Tripathi. Enhanced dielectric properties of Fe-substituted TiO₂ nanoparticles Physica B-condensed matter, 2017, Vol. 534, p.1-4.
- [49] PM Carmona-quirola, S Martinez-ramirez, HA Viles. Efficiency and durability of a self-cleaning coating on concrete and stones under both natural and artificial ageing trials. Applied surface science, 2017, Vol. 433, p. 312-320.
- [50] MAM Al-Alwani, A Mohamad, NA Ludin. Dye-sensitised solar cells: Development, structure, operation principles, electron kinetics, characterisation, synthesis materials and natural photosensitisers. Renewable and Sustainable Energy Reviews, 2016, Volume 65, p. 183-213.
- [51] K Nakata, A Fujishima. TiO₂ photocatalysis: Design and applications. Journal of Photochemistry and Photobiology C: Photochemistry Reviews, 2012, vol. 13, p. 169-189.

- [52] CO Ayieko, RJ Musembi, SM Waita, BO Aduda, PK Jain. Performance of $\text{TiO}_2/\text{In}(\text{OH})\text{iSj}/\text{Pb}(\text{OH})\text{xSy}$ Composite ETA Solar Cell Fabricated from Nitrogen Doped TiO_2 Thin Film Window Layer. *International Journal of Materials Engineering*, 2013, vol. 3(2), p. 11-16.
- [53] W Duofa, T Haizheng, Z Xiujian, J Meiyang, Z Tianjin. Enhanced photovoltaic performance in $\text{TiO}_2/\text{P3HT}$ hybrid solar cell by interface modification. *Journal of Semiconductors*, 2015, Vol. 36, No. 2.
- [54] S Saha, P Das, AK Chakraborty, R Debbarma, S Sarkar. Hybrid Solar Cell with TiO_2 Film: BBOT Polymer and Copper Phthalocyanine as Sensitizer. *Applied Physics*, 2016, vol 14, No. 3.
- [55] Z Lin, C Jiang, C Zhu, J Zhang. Development of Inverted Organic Solar Cells with TiO_2 Interface Layer by Using Low-Temperature Atomic Layer Deposition. *Mater. Interfaces*, 2013, vol. 5, p. 713–718.
- [56] A.Rapsomanikis, D.Karageorgopoulos, P.LianosE.Stathatos. High performance perovskite solar cells with functional highly porous TiO_2 thin films constructed in ambient air. *Solar Energy Materials & Solar Cells*, 2016, vol. 151, p. 36–43.
- [57] S Pitchaiya, M Natarajan, A Santhanam. Nickel sulphide-carbon composite hole transporting material for $(\text{CH}_3\text{NH}_3\text{PbI}_3)$ planar heterojunction perovskite solar cell. *Materials Letters*, 2018, vol. 221, p. 283–288.
- [58] S Bhardwaj, A Pal, K Chatterjee, TH Rana, G Bhattacharya. Significant enhancement of power conversion efficiency of dye-sensitized solar cells by the incorporation of TiO_2 -Au nanocomposite in TiO_2 photoanode. *J Mater Sci*, 2018, vol. 53, p. 8460–8473.
- [59] K Kakiage, Y Aoyama, T Yano, K Oya, J Fujisawa. Highly-efficient dye-sensitized solar cells with collaborative sensitization by silyl-anchor and carboxy-anchor dyes. *Chem. Commun*, 2015, Vol. 51, P. 15869–16002.
- [60] KH Park, CK Hong. Morphology and photoelectrochemical properties of TiO_2 electrodes prepared using functionalized plant oil binders. *Electrochemistry Communications*, 2008, vol. 10, p. 1187–1190.

- [61] R Swanepoel. Determination of the thickness and optical-constants of amorphous-silicon. J. Phys. E Sci. Instrum. 1983, vol.16, p. 1214–1222.
- [62] Film-Thickness Measurement. Global analytical and measuring instruments. Shimadzu.<https://www.shimadzu.com/an/uv/support/uv/ap/film.html> (accessed in 2018. 04)
- [63] NC Raut, T Mathews, P Chandramohan, MP Srinivasan, S Dash, AK Tyagi. Effect of temperature on the growth of TiO₂ thin films synthesized by spray pyrolysis: Structural, compositional and optical properties. Materials Research Bulletin, 2011, vol. 46, p. 2057–2063.
- [64] R. Kykyneshi, DH McIntyre, DHJ Tate, CH Park, DA Keszler. Electrical and optical properties of epitaxial transparent conductive BaCuTeF thin films deposited by pulsed laser deposition. Solid State Sciences, 2008, Vol.10, p. 921-927.
- [65] CP Lin, H Chen, A. Nakaruk, P. Koshy, CC Sorrell. Effect of annealing temperature on the photocatalytic activity of TiO₂ thin films. Energy Procedia, 2013, Vol. 34, p. 627-636.
- [66] FIM Fazli, MK Ahmad, CF Soon, N Nafarizal, AB Suriani. Dye-sensitized solar Cell using pure anatase TiO₂ annealed at different temperatures. OPTIK, 2017, Vol. 140, p. 1063-1068.
- [67] FIM. Fazli, N Nayan, MK Ahmad, ML Mohd. Effect of Annealing Temperatures on TiO₂ Thin Films Prepared by Spray Pyrolysis Deposition Method, Sains Malaysiana, 2016, Vol. 45, p.1197-1200.
- [68] P Vitanov, A Harizanova, T Ivanova. Structural and dielectric properties of TiO₂ thin films deposited by the sol-gel method on Si substrates. Journal of Physics Conference Series, 2011, vol. 356.
- [69] AS Bakri, MZ Sahdan, F Adriyanto, NA Raship, NDM Said, SA Abdullah, MS Rahim. Effect of Annealing Temperature of Titanium Dioxide Thin Films on Structural and Electrical Properties. AIP Conference Proceedings, 2017, vol. 1788.
- [70] AH Dorian. H Charles, C Sorrell. Review of the anatase to rutile phase transformation. J Mater Sci, 2011, vol. 46, p. 855–874.

- [71] P Gu, H Wu, D Yang, H Sun, P Wangyang. Influence of substrate on structural, morphological and optical properties of TiO₂ thin films deposited by reaction magnetron sputtering. *AIP Advances*, 2017, vol. 7.
- [72] S Amirtharajan, P Jeyaprakash, J Natarajan, P Natarajan. Electrical investigation of TiO₂ thin films coated on glass and silicon substrates—effect of UV and visible light illumination. *Appl Nanosci*, 2016, vol. 6, p:591–598.
- [73] MIB Bernardi, EJH Lee, PN Lisboa-Filho, ER Leite. TiO₂ Thin Film Growth Using the MOCVD Method. *Materials Research*, 2001, Vol. 4, p. 223-227.
- [74] Y Bouachiba, A Bouabellou, F Hanini, F Kermiche, A Taabouche, K Boukheddaden. Structural and optical properties of TiO₂ thin films grown by sol-gel dip coating process. *Materials Science-Poland*, 2014, Vol. 32, p. 1-6.
- [75] FD Hardcastle. Raman Spectroscopy of Titania (TiO₂) Nanotubular Water-Splitting Catalysts. *Journal of the Arkansas Academy of Science*, 2011, Vol. 65.
- [76] A Sedik, AM Ferraria, AP Carapeto, B Bellal, M Trari, Ra Outemzabet. Characterization of TiO₂ films obtained by a wet chemical process. *Journal of ELECTRICAL ENGINEERING*, 2017, VOL 68, p.31–36.
- [77] MI Khan, S Imran, MS Shahnawaz, UR Saif. Annealing effect on the structural, morphological and electrical. properties of TiO₂/ZnO bilayer thin films. *Results in Physics*, 2018, vol. 8, p. 249–252.
- [78] NR Mathews, R Erik, MA Morales, JA Cortes-Jacome. TiO₂ thin films-Influence of annealing temperature on structural, optical and photocatalytic properties *Solar Energy*, 2009, vol. 83, p. 1499–1508.
- [79] A Sedghi, NM Hoda. Influence of TiO₂ Electrode Properties on Performance of Dye-Sensitized Solar Cells. *Int. J. Electrochem. Sci.*, 2012, vol. 7, p. 12078 - 12089.
- [80] DT Chien, PD Long. Effect of annealing temperature on the structure,optical and electronic properties of TiO₂ made by thermal treatment of ti. *Communications in Physics*, Vol. 24, No. 2 (2014), pp. 155-162.



STUDY ON THE PROPERTIES OF TiO₂ THIN FILMS DEPOSITED BY ULTRASONIC SPRAY PYROLYSIS

Z. J. Chen, I. Oja Acik, I. Dündar, A. Mere
Laboratory of Thin Film Chemical Technologies
Department of Materials and Environmental Technology
Tallinn University of Technology
Ehitajate tee 5, EE-19086 Tallinn, Estonia
Phone: +372 6203369
Email: zengjunchen001@gmail.com

ABSTRACT

In present work, we have studied the structural, optical and electrical properties of TiO₂ thin films deposited at different substrates temperature for solar cell applications. Ultrasonic spray pyrolysis method was used to fabricate TiO₂ thin films because of its low-cost operation, absence of vacuum system and convenience of use. The films were sprayed from solution containing titanium(IV) isopropoxide, acetylacetone in molar ratio of 1:4 in ethanol and deposited onto substrate of microscopy glass and n-type Si (100) wafer at temperatures of 200 to 500 °C. The resulting films were annealed at 500 °C and 700 °C for 1 hour in air. The films were characterized by UV-vis spectroscopy, XRD, Raman, and I-V measurements. Results showed that the total transmittance of TiO₂ thin films decreased after annealing. The annealed film thickness increased from 80 to 510 nm with increasing deposition temperature from 200 to 500 °C. The optical properties showed the band gap for TiO₂ thin films decreased as the deposition temperature increased. As deposited films prepared below 500 °C were amorphous, whereas crystalline anatase films were obtained at 500 °C. Further annealing at 700 °C in air led to anatase crystalline formation when films were deposited below 500 °C whereas the films deposited at 500 °C consist of anatase and rutile phases.

Keywords: TiO₂, Ultrasonic spray pyrolysis, thin films

1. INTRODUCTION

Titanium dioxide (TiO₂) is one of the most important semiconductor oxides with attractive chemical, electrical, optical properties. After the first report by Fujishima and Honda (1972) on the photolysis of water by TiO₂ [1], numerous studies in the properties of nanocrystalline TiO₂ have been generated due to their promising applications in antireflection coatings [2], transparent conductors [3], dielectrics [4] and self-cleaning surfaces [5], and in solar cells, such as dye-sensitized [6], perovskite [7] or organic [8].

TiO₂ belongs to the family of transition metal oxides. It is known that TiO₂ has three crystal structures: anatase, brookite, and rutile. Anatase and rutile have a crystalline structure that corresponds to the tetragonal system while brookite has an orthorhombic crystalline structure. Rutile phase is thermodynamically stable at high temperatures. The anatase phase is metastable and transforms irreversibly to rutile at elevated temperatures [9]. The brookite phase is the rarest of the natural TiO₂ polymorphs and is the most difficult phase to prepare in the laboratory. Anatase phase has a band gap of 3.2 eV, while the rutile phase has a smaller band gap of 3.0 eV [10].

In general, anatase phase is preferred in solar cells and photocatalytic applications because anatase phase has a larger band gap, potentially higher conduction band edge energy and lower electron-hole pair recombination rate [11].



Nakaruk *et al.* [12] studied TiO₂ films deposited onto quartz substrates at 400 °C by ultrasonic spray pyrolysis method and annealed at 600 °C, 800 °C, 1000 °C show anatase phase, a mixture phase of anatase and rutile phases, and pure rutile phase, respectively. They showed also that the indirect band gap decreased from 3.54 eV to 3.26 eV and transmission of the films decreased after annealing at 600 °C and 1000 °C, respectively. Oja *et al.* [13] have reported that the phase composition of the TiO₂ films deposited by sol-gel pneumatic spray pyrolysis method is controlled by both deposition and annealing temperature. They reported that as-deposited TiO₂ films grown below 500 °C were amorphous. Only the deposition or annealing at 500 °C results in films with anatase phase and free of contaminants. Annealing at 700 °C leads to crystalline anatase if films are deposited below 400°C whereas the films grown at either 435 °C or 500 °C consist of a mixture of anatase-rutile or rutile, respectively.

Various methods have been used for preparing nanocrystalline titania, such as sol-gel [14], screen-printing [15], dip-coating [16], chemical vapor deposition [17] and ultrasonic spray pyrolysis [12,18]. Among all these methods, ultrasonic spray pyrolysis method has been drawn considerable attention due to its simplicity, cost-efficiency and convenience for fabricating TiO₂ thin films. In this paper, TiO₂ thin film was deposited on the silicon and microscopy glass substrates by ultrasonic spray pyrolysis method. The aim of this work is to deposit TiO₂ thin films at different substrate temperature and to investigate its structural, optical and electrical properties for solar cell applications.

2. METHODOLOGY

TiO₂ thin films were deposited onto microscopy glass and c-Si substrates at different substrate temperature using ultrasonic spray pyrolysis method. The precursor solution is composed of titanium(IV) isopropoxide (TTIP) as a titanium source, acetylacetonate (AcAc) as a stabilizer and ethanol as solvent. 0.2molL⁻¹ TTIP concentration and TTIP:AcAc molar ratio of 1:4 were used as starting solution. The solution was atomized by a ultrasonic generator of 1.7MHz frequency, produced aerosol was carried directly to the heated substrates using compressed air as carrier gas in a flow rate of 5 L/min and director gas (1.2 L/min) was used to adjust the spray direction. The deposition temperature (T_s) vary in the range 200 to 500 °C. The number of spray cycles were set to six.

The as-deposited films grown on glass and Si-substrates were annealed for 1 hour at 500 °C in air. The films on silicon substrates were additionally thermally treated at 700°C for 1 hour in a laboratory furnace. The structural property of the samples was investigated by X-ray diffraction (XRD) and Raman spectroscopy methods. XRD patterns were recorded by a Rigaku Ultima IV diffractometer with Cu K α radiation ($\lambda = 1.5406 \text{ \AA}$, 40 kV at 40 mA) using Si strip detector. The measurements were performed in 2 theta configurations with scan range of 20-60°, with a step of 0.02° and a scanning speed of 2°/min. The mean crystallite size was calculated by the Scherrer method from the FWHM (full width at half maximum) of the (101) peak of TiO₂ anatase phase. Raman spectra were acquired on a micro-Raman spectrometer HORIBA Jobin Yvon Model HR800 in the spectral range of 100-800 cm⁻¹ using 532 nm laser line which delivers 5 mW of power at 10 μm laser spot size during measurement.

The total transmittance of TiO₂ thin films are measured by Jasco V-670 spectrophotometer with spectral range between 250 and 1200 nm. The film thickness was calculated by using interference fringes from optical spectrum.

Current-Voltage (I-V) measurement was performed to investigate the electrical properties of TiO₂ thin film on n-Si substrate. The I-V measurement was performed with

using graphite contact and Si as a second contact. The Autolab PGSTAT 30 system was used for measuring of I-V curves of the films.

3. RESULTS AND DISCUSSION

3.1. Structural properties

3.1.1. X-ray diffraction

The XRD patterns of TiO₂ thin films on glass substrates deposited at different deposition temperatures from 200 to 500 °C are given in Fig.1. The diffraction peaks at 25.3°, 37.7°, 48.1°, 53.9° and 55.1° correspond to the (101), (004), (200), (105) and (211) anatase planes [19]. XRD studies showed that the as-deposited films prepared at substrate temperatures below 500 °C were amorphous. The anatase peak (101) becomes apparent for the films deposited at 500 °C. Annealing at 500 °C results in anatase phase for films deposited at or above 300 °C.

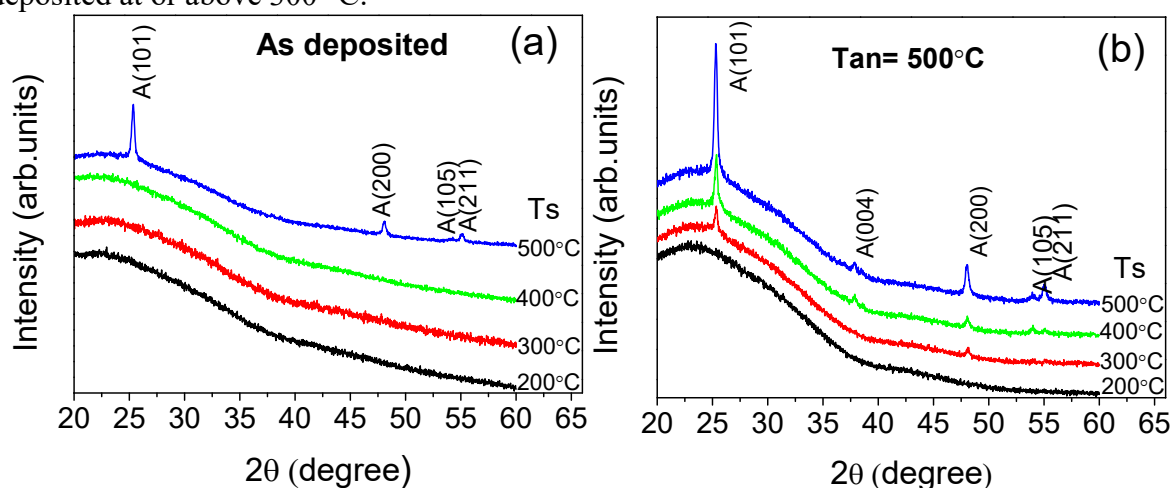


Fig.1. XRD patterns of TiO₂ thin films with glass substrates deposited at various temperatures from 200 to 500 °C: (a) as-deposited thin films, (b) thin films annealed at 500 °C.

Fig 2 shows XRD patterns of TiO₂ thin films deposited on silicon substrates. XRD result showed the films deposited at or below 300 °C were amorphous, however the films deposited at or above 400°C have anatase structure. Annealing at 500°C results in formation of anatase phase regardless of the deposition temperature. Further annealing at 700°C has significantly changed the film structure, the films deposited below or at 400 °C remain anatase, however the films deposited at 500 °C compose of the mixture of anatase and rutile phases.

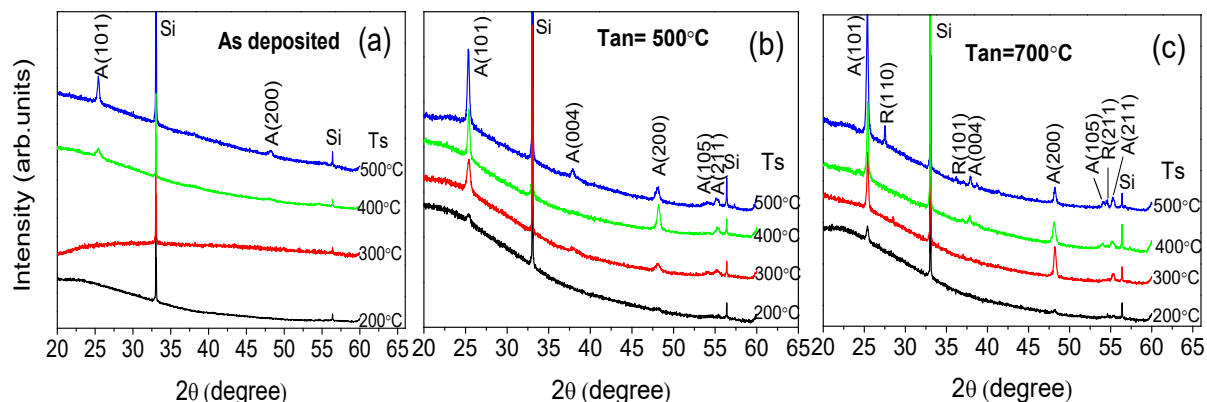


Fig.2. XRD patterns of TiO₂ thin films on silicon substrates. (a) as-deposited thin films, (b) thin films annealed at 500 °C, (c) thin films annealed at 700 °C.

The mean crystallite size of the TiO₂ films deposited onto different substrates and annealed at different temperatures were calculated by applying the Scherrer's formula [13] on the (101) anatase peak and the values obtained are presented in Table 1. The mean crystal size of anatase phase increased with the increasing deposition temperature. Annealing of TiO₂ thin films can improve their crystallinity and also increase the mean crystal size [20].

Table 1. The mean crystallite size of TiO₂ thin films deposited at different deposition temperature (T_s) and annealed at 500 °C and 700 °C.

Deposition temperature T _s (°C)	Mean crystallite size (nm)				
	Glass substrate		Silicon substrate		
	As-deposited	Annealed at 500 °C	As-deposited	Annealed at 500 °C	Annealed at 700 °C
200	-	-	-	21	30
300	-	26	-	28	37
400	-	29	17	31	40
500	28	32	31	32	42

3.1.2. Raman spectroscopy

Raman spectrum was used to further confirm the crystal phase of TiO₂ films. Fig.3 shows Raman spectra of TiO₂ films grown at different substrates and annealed at 500 °C and 700 °C. TiO₂ thin films grown onto glass substrates and annealed at 500 °C (Fig. 3a) exhibit the bands at around 142 (E_g), 197 (E_g), 398 (B_{1g}), 520 (B_{1g}) and 639 (E_g) cm⁻¹ which are assigned to TiO₂ anatase [21]. TiO₂ thin films deposited on silicon substrates and annealed at 500 °C (Fig. 3b) showed in addition the peaks at 302 and 520 cm⁻¹ belonging to the Si substrate. No rutile peaks were detected after annealing at 500 °C. TiO₂ films deposited on Si-substrate and annealed at 700 °C showed anatase phase when grown in the temperature range of 200-400 °C. However, TiO₂ films deposited at 500 °C and annealed at 700 °C showed additional Raman bands at round 232 (B_{1g}) and 440 (E_g) cm⁻¹ which belong to rutile phase [22], and thereby confirm a mixture of anatase and rutile phases in these films. The mixture phases after annealing above 700 °C have been also observed in sol-gel spin coating and ultrasonic spray pyrolysis [12-13].

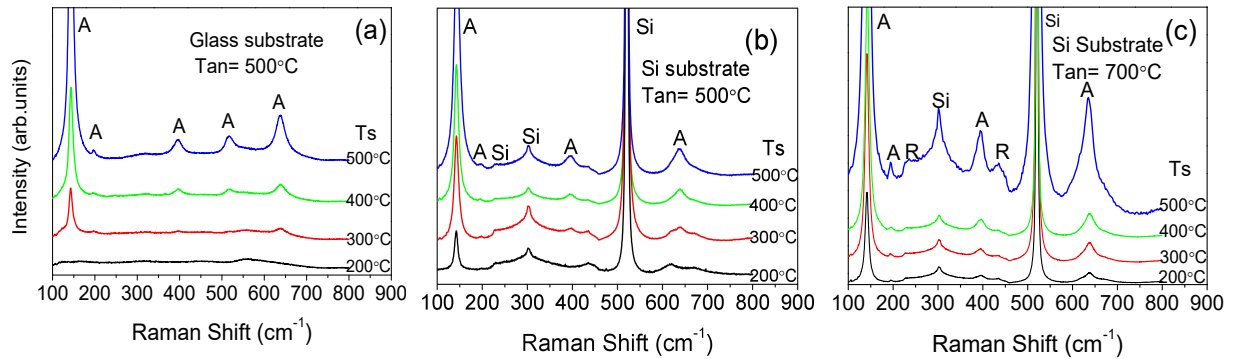


Fig.3. Raman spectrum of TiO₂ films deposited at various temperatures: (a) as-deposited films on glass substrate, (b) films deposited on Si- substrate and annealed at 500 °C, (c) films deposited on Si-substrate and annealed at 700 °C. Si means Si-substrate, A- anatase, R- rutile.

3.1.3. Optical properties

The optical transmittance spectra of TiO₂ thin films deposited onto glass substrates at temperatures from 200 to 500 °C and followed by annealing at 500 °C are presented in Fig. 4. The TiO₂ thin films were highly transparent in the visible region with transmittance above 90% for the as-deposited samples and above 80% for the annealed samples. The total transmittance decreased with increasing the deposition temperature. The interference patterns indicate the homogeneity of the films. The decrease in the optical transmittance after annealing can be related to the increase of the light diffusion with the crystallite size and particle aggregation [23].

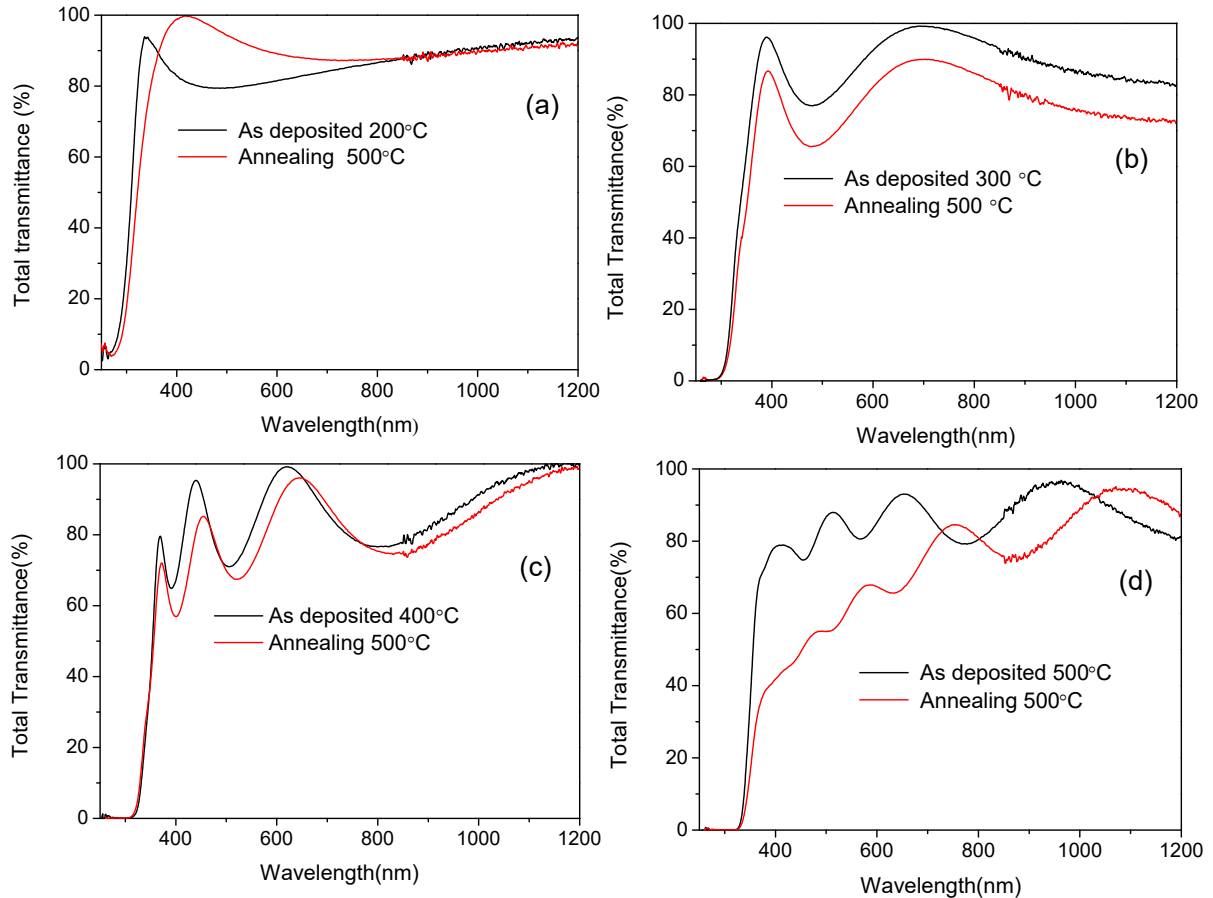


Fig.4. Total transmittance spectra of TiO₂ thin films on glass substrates: (a) as-deposited at 200 °C and followed by annealing at 500 °C, (b) as-deposited at 300 °C and followed by annealing at 500 °C, (c) as-deposited at 400 °C and followed by annealing at 500 °C, (d) as-deposited at 500 °C and followed by annealing at 500 °C

The optical band gap was determined using the Tauc expression [24],

$$\alpha = \frac{A}{h\nu} (h\nu - E_g)^n \quad (1)$$

where A is a proportionality constant, $h\nu$ is the photon energy, E_g is the band gap and $n = \frac{1}{2}$ for direct or $n = 2$ for indirect optical transitions. The optical band gap was obtained by extrapolating the linear part of the plot of $(\alpha h\nu)^2$ against $h\nu$ to the photon energy axis by assuming direct band gap is shown in Fig .5.

The band gaps of the as-deposited films were 3.46, 3.41, 3.36, 3.29 eV respectively with increasing deposition temperature from 200 to 500 °C and it decreased slightly after annealing at 500 °C, was 3.45, 3.35, 3.27 and 3.22 eV respectively. The decrease in the optical band gap of the TiO₂ films with annealing temperature might be the result of the increased crystallinity of the annealed films [20].

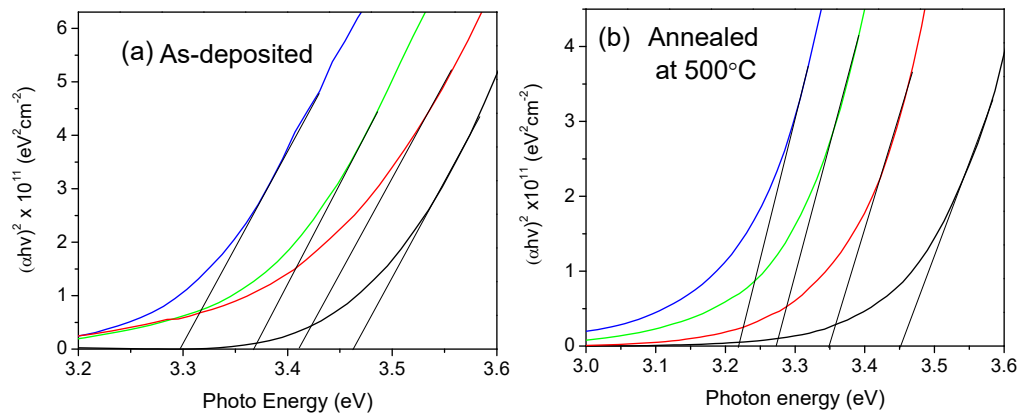


Fig .5. Band gap of TiO₂ thin films with glass substrates: (a) as-deposited films deposited at substrate temperature from 200 to 500 °C. (b) as-deposited films followed by Annealing at 500 °C.

The thickness of films on glass substrates is shown in Table 2. The thickness of as-deposited films increased from 110 to 620 nm with increasing deposition temperature from 200 to 500 °C and decreased after annealing at 500 °C. Since the solution feed rate was consistent, then it is implicit that the film thickness increased with increasing deposition temperature owing to the corresponding increase in the reaction rate. The film thickness decreases after annealing at 500 °C, compared to as-deposited films, is related with the burning out of the organic residues in the film [25].

Table 2. Film thickness of as-deposited and annealed films, deposited onto glass substrates at various substrate temperatures (T_s)

T_s (°C)	As-deposited		Annealed at 500 ° C	
	Film thickness	Band gap (eV)	Film thickness	Band gap (eV)
200	120	3.46	80	3.45
300	180	3.41	170	3.35
400	370	3.36	320	3.27
500	620	3.29	510	3.22

3.2. Electrical Resistivity

Fig. 6 shows the resistivity of the as-deposited and annealed TiO₂ films on silicon substrates. The resistivity of the films decreases with increasing deposition temperature from 200 to 300 °C, which may be due to the change of crystal structure from amorphous to crystalline anatase phase. The resistivity also decreased when increasing the annealing temperature, this phenomenon is due to increase in the grain size which leads to a decrease in the grain boundaries and hence resistivity [26].

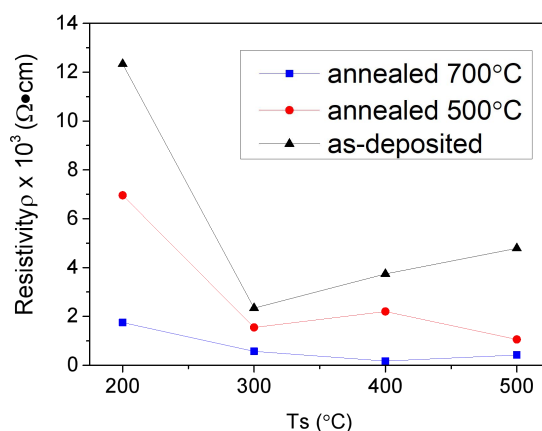


Fig.6 Resistivity of TiO₂ films deposited on silicon substrates at various substrate temperatures (Ts) and after various annealing temperatures.

4. CONCLUSION

Ultrasonic spray pyrolysis method was used to deposit TiO₂ film and the effect of deposition and annealing temperature on the structural, optical, electrical properties was investigated. The XRD data reveals that the as-deposited grown below 400°C onto glass substrate and below 300°C onto Si substrate are amorphous. Annealing at 500°C results in formation of anatase structure, if the films are deposited at temperatures ≥ 300°C onto glass substrates or in the temperature range 200-500 °C onto Si substrates. The mean crystallite size of anatase structure remains in the range of 20-32 nm irrespective of the deposition, annealing temperature and substrate. Further annealing of TiO₂ films on Si substrate at 700 °C led to the formation of the mixture of anatase and rutile phase if deposited at 500 °C and increase in the average crystallite size of the anatase structure to the range of 30-40 nm. As-deposited TiO₂ films show high optical transmittance and band gap values in the range of 3.5-3.3 eV if deposited at 200-500 °C. Film thickness was found to increase with deposition temperature and decrease after annealing at 500 °C. The resistivity of TiO₂ films depends on the deposition temperature and was found to decrease with increasing the annealing temperature. The films deposited above 300 °C and annealed at 500 °C are applicable as window layer in solar cell devices and will be tested in further research.

5. ACKNOWLEDGEMENT

This study was financially supported by the Estonian Ministry of Education and Research project IUT19-4, and by the European Union through the European Regional Development Fund project TK141 “Advanced materials and high-technology devices for energy recuperation systems”.

6. REFERENCES

- [1]. KOHTANI, S., KAWASHIMA, A., MIYABE, H. Reactivity of Trapped and Accumulated Electrons in Titanium Dioxide Photocatalysis. *Catalysts*, 2017, Vol. 7.



- [2]. RODRIGUEZ, DF., PERILLO, PM., BARRERA, MP. High performance TiO₂ nanotubes antireflection coating. *Materials science in semiconductor processing*, 2017, Vol.71, p.427-432.
- [3]. SINGH, S., SHARMA, V., SACHDEV, K. Investigation of post annealing effects on Nb: TiO₂ transparent conducting thin films. *Advanced science letters*, 2016, Vol. 22, p. 3773-3776.
- [4]. ALI, T., AHMED, A., SIDDIQUE, MN., TRIPATHI, P. Enhanced dielectric properties of Fe-substituted TiO₂ nanoparticles *Physica B-condensed matter*, 2017, Vol. 534, p.1-4.
- [5]. CARMONA-QUIROGA, PM., MARTINEZ-RAMIREZ, S., VILES, HA. Efficiency and durability of a self-cleaning coating on concrete and stones under both natural and artificial ageing trials. *Applied surface science*, 2017, Vol. 433, p. 312-320.
- [6]. MA, QL., MA, SQ., HUANG, YM. Enhanced photovoltaic performance of dye sensitized solar cell with ZnO nanohoneycombs decorated TiO₂ photoanode. *Materials letters*, 2018, Vol. 218, p. 237-240.
- [7]. NOURI, E., MOHAMMADI, MR., XU, ZX., DRACOPOULOS, V., LIANOS, P. Improvement of the photovoltaic parameters of perovskite solar cells using a reduced-graphene-oxide-modified titania layer and soluble copper phthalocyanine as a hole transporter. *Physical chemistry chemical physics*, 2018, Vol, 20, p. 2388-2395.
- [8]. LIRA-CANTU, M., CHAFIQ, A., FAISSAT, J., GONZALEZ-VALLS, I., YU, YH. Oxide/polymer interfaces for hybrid and organic solar cells: Anatase vs. Rutile TiO₂. *Solar energy materials and solar cells*, 2011, Vol.95, p.1362-1374.
- [9]. MAHALINGAM, S., EDIRISINGHE, MJ. Characteristics of electrohydrodynamically prepared titanium dioxide films. *Applied physics a-materials science & processing*, 2007, Vol. 89, p. 987-993.
- [10]. PAUL, S., CHOUDHURY, A. Investigation of the optical property and photocatalytic activity of mixed phase nanocrystalline titania. *Applied nanoscience*, 2014, Vol. 4, p.839-847.
- [11]. LUTTRELL, T., HALPEGAMAGE, S., TAO, JG., KRAMER, A., SUTTER, E., BATZILL, M. Why is anatase a better photocatalyst than rutile? - Model studies on epitaxial TiO₂ films. *Scientific reports*, 2014, Vol. 4, No. 4043.
- [12]. NAKARUK, A., RAGAZZON, D., SORRELL, CC. Anatase-rutile transformation through high-temperature annealing of titania films produced by ultrasonic spray pyrolysis. *Thin solid films*, 2010, Vol. 518, p. 3735-3742.
- [13]. OJA, I., MERE, A., KRUNKS, M., NISUMAA, R., SOLTERBECK, CH., ES-SOUNI, M. Structural and electrical characterization of TiO₂ films grown by spray pyrolysis. *Thin solid films*, 2006, Vol. 515, p. 674-677.
- [14]. YU, JG., ZHAO, XJ., ZHAO, QN. Effect of surface structure on photocatalytic activity of TiO₂ thin films prepared by sol-gel method. *Thin solid films*, 2000, Vol. 379, p. 7-14.
- [15]. WATANABE, F., MOTODA, S., MORITA, M. Photo-Potential Property of TiO₂ Electrode Prepared by the Screen Printing Method. *Batteries and energy technology joint general session*, 2017, Vol. 75, p. 93-100.
- [16]. NEGISHI, N., TAKEUCHI, K. Preparation of TiO₂ thin film photocatalysts by dip coating using a highly viscous solvent. *Journal of sol-gel science and technology*, 2001, Vol. 22, p. 23-31.
- [17]. SUN, HF., WANG, CY., PANG, SH., LI, XP., TAO, Y., TANG, HJ., LIU, M. Photocatalytic TiO₂ films prepared by chemical vapor deposition at atmosphere pressure. *Journal of non-crystalline solids*, 2008, Vol. 354, p. 1440-1443.



- [18]. ENNACERI, H., BOUJNAH, M., TALEB, A., KHALDOUN, A., SAEZ-ARAOZ, R., ENNAOUI, A., EL KENZ, A., BENYOUSSEF, A. Thickness effect on the optical properties of TiO₂-anatase thin films prepared by ultrasonic spray pyrolysis: Experimental and ab initio study. *International journal of hydrogen energy*, 2017, Vol. 42, p. 19467-19480.
- [19]. FAZLI, FIM., AHMAD, MK., SOON, CF., NAFARIZAL, N., SURIANI, AB., MOHAMED, A., MAMAT, MH., MALEK, MF., SHIMOMURA, M., MURAKAMI, K. Dye-sensitized solar Cell using pure anatase TiO₂ annealed at different temperatures. *OPTIK*, 2017, Vol. 140, p. 1063-1068.
- [20]. C-P, LIN., H. CHEN, A. NAKARUK, P. KOSHY, C.C. SORRELL. Effect of annealing temperature on the photocatalytic activity of TiO₂ thin films. *Energy Procedia*, 2013, Vol. 34, p. 627-636.
- [21]. BOUACHIBA, Y., BOUABELLOU, A., HANINI, F., KERMICHE, F., TAABOUCHE, A., BOUKHEDDADEN, K. Structural and optical properties of TiO₂ thin films grown by sol-gel dip coating process. *Materials Science-Poland*, 2014, Vol. 32, p. 1-6.
- [22]. JUMA, AO., ACIK, IO., MIKLI, V., MERE, A., KRUNKS, M. Effect of solution composition on anatase to rutile transformation of sprayed TiO₂ thin films. *Thin solid films*, 2015, Vol. 594, p. 287-292.
- [23]. BEN KAROUI, M., KADDACHI, Z., GHARBI, R. Optical properties of nanostructured TiO₂ thin films. TUNISIA-JAPAN SYMPOSIUM, 2015, R&D of Energy and Material Sciences for Sustainable Society. [CD]. Gammarth, TUNISIA, 2014 NOV 28-30.
- [24]. TAUC, J. Optical properties and electronic structure of amorphous Ge and Si. *Physica status solidi (b)*, 1966, vol. 15, p. 627-637.
- [25]. Oja, I., Mere, A., Krunks, M., Solterbeck, C-H., Es-Souni, M. Properties of TiO₂ Films Prepared by the Spray Pyrolysis Method. *Solid State Phenomena*, 2004, Vol. 99-100, p. 259-264.
- [26]. BAKRI, AS. Effect of Annealing Temperature of Titanium Dioxide Thin Films on Structural and Electrical Properties. ICESNANO 2016, International Conference on Engineering, Science and Nanotechnology. [CD]. Solo, Indonesia. 2016 Aug 03-05.